Localization with Joint Diffusion-based Molecular Communication and Sensing Systems: Fundamental Limits and Tradeoffs

Flavio Zabini, *Member, IEEE*

***Abstract*—This paper introduces and examines a novel joint communication and sensing system based on molecular diffusion. Using a configuration of at least four fully absorbing spherical receivers, the proposed system achieves precise 3D-localization of a pointwise transmitter by counting the same molecules emitted for communication purposes. We develop an analytical framework to explore the fundamental limits of communication and localization within this context. Exact closed-form expressions for the bit error probability and the Cramér-Rao bound on localization error are derived, considering both Poisson concentration and timing transmitter models, with and without accounting for molecule degradation. For the first time, theoretical trade-offs between communication and localization performance are established, taking inter-symbol interference and molecule degradation into account. In scenarios without molecule degradation, inter-symbol interference detrimentally affects communication but enhances localization. Conversely, the introduction of degradation improves communication performance but partially compromises localization effectiveness. These trade-offs are navigated by adjusting number of transmitted symbols or degradation rate, respectively. Furthermore, we compare communication and localization ranges, alongside the associated costs measured in terms of average emitted molecules required to meet performance requirements.**

***Index Terms*—Joint molecular communication and sensing, 3D localization, bit error probability, Cramér-Rao bounds, molecule degradation**

I. Introduction

THE INTEGRATION of communication and sensing functions is becoming increasingly crucial in the realms of 5G, 6G, and IoT, with a myriad of papers published in recent years addressing the so-called Joint communication and sensing (JCS) systems [1]–[6]. Strictly speaking, this term refers to a system wherein the same waveform serves both to convey information and to provide sensing functions such as passive target localization [7]–[9]. This feature will be increasingly essential in future communication systems, as it enables the addition of the ever more demanded sensing function without necessitating additional resource expenditure in terms of, for instance, occupied bandwidth and emitted power. In light of this evidence, one may wonder if something similar can be achieved even in micro- or nano-scale communication systems, such as molecular ones, where the resource to be "saved" is constituted by the number of transmitted molecules.

This work was submitted in part at the IEEE International Symposium on Information Theory (ISIT 2024).

This work has been carried out in the framework of the CNIT National Laboratory WiLab. F. Zabini is with DEI and WiLab, University of Bologna/CNIT, Italy, email: f.zabini@ieee.org.

Unlike electromagnetic and acoustic communications, which rely solely on waves, and optical and quantum communications, which involve both wave and particle properties, molecular communications are particle-based in nature [10]–[12]. Moreover, in this case, it is not necessary to spend energy on transmission, as information-carrying molecules are conveyed by the fluid's Brownian motion. However, the negative aspect is the inherent unpredictability associated with this random motion. In electromagnetic and acoustic communications, noise is usually represented by a source independent of the useful signal, e.g., additive white Gaussian noise (AWGN). Thus, increasing the power improves the signal-to-noise ratio (SNR). In molecular communication via diffusion (MCvD), however, the signal itself is intrinsically affected by random disturbances. More specifically, if the information is encoded in the local concentration of information-carrying molecules (i.e., in the number of molecules observed by a certain model of receiver in certain volume within a certain time), the signal results in a random process (or, equivalently, a random variable (RV) if a given time instant is considered).

It is demonstrated in [13] that the number of emitted molecules can be modeled by a Poisson RV. Moreover, it is shown in [10], [14] that also the number of received molecules after diffusion is a Poisson RV. The pioneering study conducted by [15] investigated the capacity of the MCvD channel. Nevertheless, the attainment of theoretical capacity values presents obstacles due to inter-symbol interference (ISI) originating from the high temporal correlation inherent in the molecular channel. Unfortunately, unlike in electromagnetic communications, in molecular communications, the utilization of a counterpart to raised cosine equalization is not feasible. Primarily, this is because, due to the particle-based nature of this communication paradigm, the number of received molecules (upon which information encoding relies, such as in the case of on-off keying (OOK) modulation) follows a Poisson distribution, rendering any physical significance to filtering that entails negative values meaningless. However, this does not imply that ISI cannot be at least partially mitigated using alternative signal processing techniques, such as power adjustment techniques [16], or physically realizable frequency filtering approaches [17].

In a point-to-point MCvD, thanks to the Poisson nature of the observation variable, the evaluation of the average number of received molecules (first order analysis) is sufficient to quantify the effectiveness of the communication (see, e.g., [18], where the bit error probability (BEP) is evaluated con-

sidering a programmed molecule degradation to mitigate ISI). If, instead, there are multiple transmitters randomly positioned in space (referred to as "large scale molecular communication systems", see [19]–[22]), it can be demonstrated that a second-order statistical analysis is necessary.[1].

In such systems, it is analytically demonstrated in [22] that the theoretically optimal approach to enhance transmission reliability (by mitigating both the effects of molecular noise and ISI) is to increase the density of transmitters.[2] However, due to physical constraints related to the finite number of chemical receptors on the surface of an actual receiver, the quantity of absorbable molecules per unit time is limited [23]–[25]. Exceeding a certain threshold in the number of transmitters (and consequently, the amount of molecules to be received) results in a saturation effect that renders communication infeasible [26].

At this stage, it is worth exploring whether, in addition to its communication functionality, that is constrained by the aforementioned issues, molecular diffusion could serve another joint purpose, such as microscale localization or sensing.
The emission of molecules represents a form of nanoscale communication inherently poised for utilizing molecules to transmit information between nanoscale devices (as seen in the referenced papers) and for developing sensors based on molecular communication principles for various applications such as environmental monitoring or medical diagnostics [27]. Applications of molecular communication in the biomedical field encompass drug delivery (utilizing molecules to transport drugs to precise targets within the body) [28], health monitoring (tracking biochemical markers within the body for early disease detection) [29], and implant communication (establishing communication between implanted medical devices using molecules as messengers) [30]. Moreover, within the realm of synthetic biology, there is ongoing research into developing biosensors that leverage molecular communication to detect specific molecules in the environment or within biological systems [31].

Many papers discussed in [32] explore practical applications where molecules emissions (unrelated to transmitting information bits) can be used for anomaly detection or localization. Anomaly detection relies on both stationary and mobile sensors. Stationary sensors employ non-cooperative and cooperative methods. For instance, a single sensor detects virus-laden aerosols [33], while multiple sensors and a fusion center enhance monitoring [34]. Mobile sensors are primarily used in cooperative detection, aiding in early cancer detection in the circulatory system [35] and monitoring pipeline abnormalities [36]. Anomaly localization is a step further with respect detection. Stationary sensors employ various techniques, while mobile sensors can be propelled or non-propelled, each offering distinct benefits. Application-centric frameworks, such as touch communication for drug delivery [37] and tumor detection with external devices [38], improve anomaly management. The sensors have the capability to release molecules, either singly or in multiple types, for diverse functions. For instance, they can be utilized for inter-sensor communication and communication with the fusion center [36], as well as for the targeted delivery of drug molecules [39]. These molecules might be stored within the sensor's storage or synthesized by the sensor through chemical processes. The process of molecule release is regulated by the sensor itself, which can be achieved through mechanisms such as ion channels [40] and ion pumps [41].

The initial exploration of utilizing molecule transmission to localize a target represented by a nanomachine is evident in previous works like [42], [43]. However, these studies primarily focus on estimating the distance from the target rather than directly determining its position, given the challenges posed by the chaotic nature of Brownian motion.

In [44], target localization is achieved through distance estimation within a constrained scenario resembling 'vessel-like' diffusion, as opposed to diffusion in an ideal fluid without limitations. The early endeavors to evaluate localization performance in a three-dimensional diffusion-based context are documented in [45]–[47]. While [45] lacks analytical results, [46] introduces a generalized Cramér-Rao bound (CRB), although it relies on a Gaussian approximation for the number of received molecules. This approximation, as cautioned in [18], may introduce inaccuracies, particularly noticeable when transmitted molecules are scarce, potentially distorting the bound. Finally, [48] is prompted by the challenge of utilizing molecular communication for signaling and localizing anomalies that emit insufficient molecules. It explores a two-dimensional scenario, potentially extendable to three dimensions. The assessment metric employed revolves around the probability of correct or incorrect localization, with no explicit evaluation of a genuine communication function (e.g., bit transmission).

In contrast to the approaches taken in [48] and the studies outlined in [32], we consider a scenario where an emitter (biological or artificial) releases molecules to transmit bits of information to a certain number of receivers. These receivers precisely localize the emitter due to this emission, which would occur regardless. This is why we refer to it as joint communication and sensing. The motivation for the present work stems from the observation that in numerous previously cited studies within the literature nanomachines communicate by emitting molecules [15]–[26], and these emissions are solely used for communication purposes, typically the transmission of bits of information. We propose to also utilize these molecular emissions for localizing the emitter, which is feasible in a 3D environment if there are at least four collaborating receivers. Our investigation directly addresses the fundamental question: "What are the joint performance limits of molecular communication and localization?" Our objective is to discern these limits while adjusting various system parameters. More specifically, our contributions are as follows:

[1]This is because the randomness of the transmitter-receiver distance affects the overall statistics of received molecules, which are no longer Poisson [22]

[2]Intuitively, this can be explained as follows: when the transmitters density is very high, the distance between the receiver and the nearest transmitter is very small and, this, the contribution of that transmitter dominates over all others. Since it is very close, it has a greatly reduced ISI contribution (because the arrival delay of molecules rarely exceeds the symbol time) and a reduced probability that the transmitted molecules do not reach the receiver (because the distance they must travel via Brownian motion is small).

- Regarding the communication aspect, we extend the analytical framework proposed by [18] to include the case of a Poisson timing transmitter (with rectangular intensity function). This extension is essential because a nanomachine transmitting molecules for localization may not always emit all of them at the beginning of the time symbol [47].
- Concerning the localization aspect, we develop a novel analytical framework by completely reformulating the method used in anchor-based 3D radar localization [49] to suit the vastly different molecular diffusion scenario. This CRB calculation methodology was first proposed by us in [50], where, however, the communication function was completely absent.[3]
- We derive exact and closed-form expressions for the BEP in digital transmission and the CRB on target localization error, for both Poisson concentration and timing transmitter models, without resorting to any Gaussian approximation as seen in previous literature.

Leveraging the analytical framework, we are now able to investigate the fundamental limits of joint molecular communication and sensing for the first time. This includes comparing communication and localization ranges, as well as assessing the efficiency of both tasks in terms of the average number of emitted molecules required to achieve a target performance level. By examining the opposing effects of factors such as ISI and molecular degradation on communication and localization performance, we derive tradeoff figures essential for understanding the fundamental limits of JCS. This enables us to quantify how much the BEP increases if a localization error not exceeding a certain threshold is required, or vice versa.

The paper is organized as follows. In Sec. II, the system model is described. In Sec. III and Sec. IV, analytical expressions for, respectively, the BEP and the CRB on target localization error of the considered JCS molecular system are obtained for both Poisson concentration and timing transmitter models. In Sec. V numerical results for a case study are discussed based on the closed forms previously derived. Finally, in Sec. VI conclusions are drown

II. System Model

We consider a joint molecular communication and sensing system like that sketched in Fig. 1. The environment considered is an ideal fluid unlimited in three dimensions. The target to be localized is a pointwise transmitter which emits molecules for communication purposes according to a Poisson concentration or timing model (see Fig. 2). The system is constituted by $L \geqslant 4$ fully absorbing spherical receivers which can cooperate to perform anchor-based 3D localization using range measurements. Measurements are done based on the number of molecules received. Each receiver can autonomously decode the information delivered by the emitted molecules for the communication task. We assume that each spherical fully absorbing receiver is sufficiently far apart from the others so that the mutual reduction effect on the hitting rate of each receiver, investigated in [17] and [51], is negligible.[4]

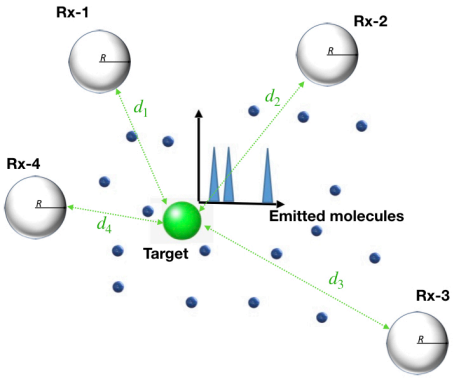

Fig. 1. Sketch of the proposed joint molecular communication and sensing system.

A. Brownian motion and absorption process

The main source of randomness in molecular communications via diffusion is the Brownian motion of molecules themselves, that can be described stochastically thanks to Fick's law of diffusion. Here we define the function $F_{\text{hit}}(d,t)$, which describes the fraction of molecules received (i.e., the probability that the emitted molecules is received) at distance r from the point transmitter till time t , provided that the emission takes place at the time origin and $t \geqslant 0$. This function depends on the receiver model and on the way of considering finite molecule's lifetime.

1) Fully absorbing receiver without molecule degradation: According to [52], the fraction of molecules received by a spherical fully absorbing receiver (with radius R) at distance d from the point transmitter till time t is given by

$$F_{\text{hit}}(d,t) = \frac{R}{d}\text{erfc}\left(\frac{d-R}{\sqrt{4Dt}}\right) , \tag{1}$$

where D is the diffusion coefficient (in m^2/s, see, e.g., [53]), provided that the emission happens at the time origin and $t \geqslant 0$.[5] We assume that each information molecule undergoes its own separate diffusion and absorption processes. This allows us to apply the superposition of effects.

The so-called hitting rate is defined as the derivative of (1) with respect to the time:

$$f_{\text{hit}}(d,t) = \frac{R}{d}\frac{1}{\sqrt{4\pi Dt}}\frac{d-R}{t}\exp\left[-\frac{(d-R)^2}{4Dt}\right] . \tag{2}$$

As is known, $f_{\text{hit}}(d,t)$ represents the (infinitesimal) probability that a molecule emitted at the time origin at distance d is received (exactly) at time t. The probability that a molecule

[3]In fact, in [50], the transmitter to be localized emits molecules continuously (according to the propensity function of an autocatalytic reaction), while here the emission follows the pattern of a PAM signal that transmits information bits, according to (20).

[4]This happens when the minimum distance between the fully absorbing receivers is greater than 1-2 orders of magnitude compared to the radius R of the receivers themselves.

[5]For $t < 0$ it is $F_{\text{hit}}(r,t) = 0$ since no molecule can be received before the emission.

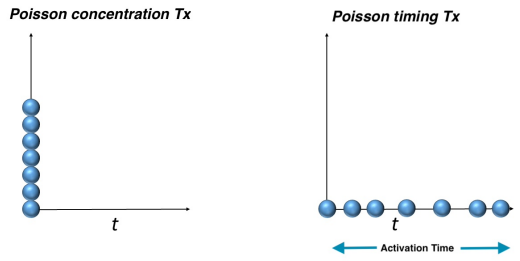

Fig. 2. Poisson concentration transmitters emit all molecules at $t = 0$. Poisson timing transmitters emit molecules one-by-one at random instants [22].

emitted at $t = 0$ is observed within the interval $[t_0, t_0 + T_0]$ is thus given by

$$\int_{t_0}^{t_0+T_0} f_{\text{hit}}(d,t)dt = \overline{F}_{T_0}(d,t_0)\,, \tag{3}$$

where

$$\overline{F}_{T_0}(d,t) \triangleq F_{\text{hit}}(d,t+T_0) - F_{\text{hit}}(d,t)\,. \tag{4}$$

The time invariance of the Fick's law of diffusion allows us to write that, if the emission happens at τ_0, the probability that a molecule is received in the interval $[t_0, t_0 + T_0]$ is

$$\overline{F}_{T_0}(d,t_0-\tau_0) = F_{\text{hit}}(d,t_0+T_0-\tau_0) - F_{\text{hit}}(d,t_0-\tau_0)\,. \tag{5}$$

2) Fully absorbing receiver with molecule degradation: By taking the molecule degradation into account, the fraction of molecules received within time t becomes [19]:

$$\begin{aligned} F_{\text{hit}}(d,t) = {} & \frac{R}{d}e^{-\sqrt{\frac{k_{\text{d}}}{D}}(d-R)} - \frac{R}{2d}e^{-\sqrt{\frac{k_{\text{d}}}{D}}(d-R)} \\ & \cdot \left[\text{erf}\left(\frac{d-R}{\sqrt{4Dt}} - \sqrt{k_{\text{d}}t}\right) + e^{2\sqrt{\frac{k_{\text{d}}}{D}}(d-R)}\right. \\ & \left. \cdot \left(\text{erf}\left(\frac{d-R}{\sqrt{4Dt}} + \sqrt{k_{\text{d}}t}\right) - 1\right) + 1\right]\,, \end{aligned}$$

where k_{d} is the molecule degradation rate. For future purposes, we can re-write such expression in a more convenient form as:

$$\begin{aligned} F_{\text{hit}}(d,t) = {} & \frac{R}{2d}\, e^{\sqrt{\frac{k_{\text{d}}}{D}}(d-R)}\text{erfc}\left(\frac{d-R}{\sqrt{4Dt}} + \sqrt{k_{\text{d}}t}\right) \\ & + \frac{R}{2d}\, e^{-\sqrt{\frac{k_{\text{d}}}{D}}(d-R)}\text{erfc}\left(\frac{d-R}{\sqrt{4Dt}} - \sqrt{k_{\text{d}}t}\right)\,, \end{aligned} \tag{6}$$

that easily reduces to (1) for $k_{\text{d}} = 0$. The probability that a molecule is received in the interval $[t_0, t_0+T_0]$ is still formally described by (5), but with (1) replaced by (6) in (4).

B. Transmitter models

1) Reception with Poisson concentration transmitter: If a deterministic number of molecules were emitted at a certain time (e.g., $t = 0$, without loss of generality) no randomness would be obviously introduced in the emission process (exact concentration model). However, according to the chemical-physical reasons explained in [13] (the molecules are the products of certain reactions that occur randomly.),[6] the number of emitted molecules is a RV (e.g., Poisson concentration transmitter) [54]. In the Poisson concentration model, the number n_{Tx} of emitted molecules at $t = 0$ is not deterministic, but it is modeled by a Poisson RV with mean N_{Tx}. Each of the n_{Tx} molecules has probability $F_{\text{hit}}(d,t)$ of being received at a distance d till time t. More formally, the diffusion process of the n-th molecule can be stochastically described (for given d and t) by the Bernoulli RV $\mathsf{b}_n|_{d,t}$

$$\mathsf{b}_n|_{d,t} \sim \mathcal{B}[F_{\text{hit}}(d,t)]\,, \tag{7}$$

which takes value 1 if the n-th emitted molecule is received and 0 otherwise.

However, unlike the exact case, the number $\mathsf{a}|_{d,t}$ of received molecules at distance d till time t is no more a binomial RV, but it is given by the random sum of the aforementioned Bernoulli RVs

$$\mathsf{a}|_{d,t} = \sum_{n=1}^{\mathsf{n}_{\text{Tx}}} \mathsf{b}_n|_{d,t}\,, \tag{8}$$

where $\mathsf{b}_n|_{d,t}$ can be considered as independent identically distributed (IID) due to the assumption of independent diffusion of each information molecule.

If $F_{\text{hit}}(d,t)$ were equal to 1, (8) would result in a Poisson RV with average N_{Tx}. Due the (independent) retention process and the properties of the Poisson RV,[7] in the general case we still obtain a Poisson RV with average:

$$\begin{aligned} \mathbb{E}\left\{\mathsf{a}|_{d,t}\right\} &= \mathbb{E}\left\{\sum_{n=1}^{\mathsf{n}_{\text{Tx}}} \mathsf{b}_n|_{d,t}\right\} = \mathbb{E}\left\{\sum_{n=1}^{\mathsf{n}_{\text{Tx}}} F_{\text{hit}}(d,t)\right\} \\ &= N_{\text{Tx}}F_{\text{hit}}(d,t)\,, \end{aligned} \tag{9}$$

where the first equality comes from the substitution of (8), the second from taking the average over $\mathsf{b}_n|_{d,t}$, which has mean $F_{\text{hit}}(d,t)$, and the third from summing equal identical terms and averaging over n_{Tx}. According to (3) and (5), if the emission happens at τ_0 (instead of at 0) and if the observation is done in the interval $[t_0, t_0+T_0]$ (instead of $[0,t]$), $F_{\text{hit}}(d,t)$ has to be replaced by $\overline{F}_{T_0}(d,t_0-\tau_0)$ and the number of received molecules results to be distributed as:[8]

$$\mathsf{a}[t_0,t_0+T_0]_{\tau_0}^{(\text{con})} \sim \text{Pois}\left[N_{\text{Tx}}\overline{F}_{T_0}(d,t_0-\tau_0)\right]\,, \tag{10}$$

where by $\text{Pois}(\lambda)$ we indicate the Poisson distribution with parameter λ.

[6]Each molecule to be emitted in the interval $[t, t+\tau]$ is produced by a reaction of a certain type that occurs independently of the others (of the same type), but with the same probability (determined by the propensity function of the reaction itself). Therefore, the number of molecules that can be emitted in the interval $[t, t+\tau]$, being the sum of independent Bernoulli RVs, which take the value zero if the reaction does not occur and one if it does (with the probability given by the propensity function), follows a Poisson distribution.

[7]The sum of independent Poisson RV is still Poisson.

[8]Here, the superscript "(con)" stands for "concentration model", as well as, in the following subsection, "(tim)" will stand for "timing model".

2) Reception with Poisson timing transmitter model: According to the timing transmitter model, the transmitter releases individual molecules one by one, at specified time instances. If such instants are unknown a priori, they can be modeled by RVs. When emission times are independent of each other, they can be considered as instantiations of a temporal (generally, non-stationary) Poisson point process (PPP) Π with intensity $\lambda_{\text{Tx}}(t)$.[9]

Formally, the n-th molecule is emitted at the random time $\tau_n \in \Pi$ and thus can be described (given d, t) by the Bernoulli RV

$$\mathsf{b}_n|_{d,t} \sim \mathcal{B}[F_{\text{hit}}(d, t-\tau_n)] \,, \tag{11}$$

where $F_{\text{hit}}(d, t-\tau_n)$ (thanks to the time invariance of Fick's law) represents the probability of being received at distance d till time t. As a consequence, the number of received molecules at distance d till time t is given by the random sum

$$\mathsf{a}|_{d,t} = \sum_{n \in \mathcal{I}\{\Pi\}} \mathsf{b}_n|_{d,t} \,, \tag{12}$$

where $\mathcal{I}\{\Pi\}$ indicates the index set of Π.

By comparing (12) to (8), it can be noticed that the Poisson concentration model can be derived as a special case of Poisson timing transmitter model where Π is a PPP with $\lambda_{\text{Tx}}(t) = N_{\text{Tx}}\delta(t)$ in the sense of distributions.

If $F_{\text{hit}}(d, t-\tau_n)$ were equal to 1 for all n, (12) would result in a sum of "ones" arriving as the points belonging to a PPP with intensity $\lambda(t)$, that is a Poisson RV. Due to the (independent) retention process and the properties of a PPP,[10] in the general case we still obtain a Poisson RV with average:

$$\begin{aligned}\mathbb{E}\{\mathsf{a}|_{d,t}\} &= \mathbb{E}\Big\{\sum_{n\in\mathcal{I}\{\Pi\}} \mathsf{b}_n|_{d,t}\Big\} = \mathbb{E}\Big\{\sum_{n\in\mathcal{I}\{\Pi\}} F_{\text{hit}}(d, t-\tau_n)\Big\} \\ &= \int_0^{+\infty} \lambda_{\text{Tx}}(\tau) F_{\text{hit}}(d, t-\tau) d\tau \,,\end{aligned} \tag{13}$$

where the first equality arises from substitution (12), the second from averaging over $\mathsf{b}_n|_{d,t}$, which has a mean $F_{\text{hit}}(d, t-\tau)$, and the last from applying Campbell's theorem, [55]–[57] recalling that τ_n belongs to the PPP Π, which has intensity function $\lambda_{\text{Tx}}(\cdot)$. According to (3), if the observation is done in the interval $[t_0, t_0+T_0]$, instead of $[0, t]$, $F_{\text{hit}}(d, t)$ has to be replaced by $\overline{F}_{T_0}(d, t_0)$ and the number of received molecules due to the transmission with intensity $\lambda_{\text{Tx}}(\cdot)$ results to be distributed as:

$$\mathsf{a}[t_0, t_0+T_0]^{(\text{tim})}_{\lambda_{\text{Tx}}} \sim \text{Pois}\left[\int_0^{+\infty} \lambda_{\text{Tx}}(\tau)\overline{F}_{T_0}(d, t_0-\tau) d\tau\right] . \tag{14}$$

III. Communication functionality

As for communication purposes, d is intended as the distance between the transmitter and one of the receivers we arbitrarily consider for studying point-to-point transmission. We consider transmitting $K+1$ bits with an OOK modulation and denote as $\mathsf{d}_k \in \{0, 1\}$ the value of the k-th bit, with $\{kT_{\text{b}}\}$ with $k = \{0, 1, \cdots, K\}$. Let p_0 be the probability that the k-th transmitted bit is 0 and $p_1 = 1-p_0$ be the probability that it is 1. Without loss of generality we focus on the last transmitted bit d_K.

A. Bit data transmission and decision variable

1) Data transmission with Poisson concentration transmitter: In the case of Poisson concentration transmitter, molecules emissions occur at time instants kT_{b} (T_{b} is the bit time). Thus, by using (10) with $t_0 = KT_{\text{b}}$, $T_0 = T_{\text{b}}$, and $\tau_0 = kT_{\text{b}}$, due to the superpositions of effects, the number of molecules received in the interval $[KT_{\text{b}}, (K+1)T_{\text{b}}]$ can be written as:

$$\mathsf{c}_{\text{tot}} = \mathsf{d}_K \mathsf{a}[KT_{\text{b}}, KT_{\text{b}}+T_{\text{b}}]^{(\text{con})}_{KT_{\text{b}}} + \mathsf{c}_{ISI} \tag{15}$$

where

$$\mathsf{c}_{ISI} \triangleq \sum_{k=0}^{K-1} \mathsf{d}_k \mathsf{a}[KT_{\text{b}}, KT_{\text{b}}+T_{\text{b}}]^{(\text{con})}_{kT_{\text{b}}} \tag{16}$$

and $\{\mathsf{a}[KT_{\text{b}}, KT_{\text{b}}+T_{\text{b}}]^{(\text{con})}_{kT_{\text{b}}}\}$ result to be independent Poisson RVs with parameters:

$$\lambda_k \triangleq \mathbb{E}\left\{\mathsf{a}[KT_{\text{b}}, KT_{\text{b}}+T_{\text{b}}]^{(\text{con})}_{kT_{\text{b}}}\right\} = N_{\text{Tx}}\overline{F}_{T_{\text{b}}}(d, KT_b - kT_{\text{b}}) \,. \tag{17}$$

For the properties of the Poisson RVs,[11] we can write the probability mass function (PMF) of c_{tot} conditioned to d_K as:

$$\text{Prob}\{\mathsf{c}_{\text{tot}} = m|_{\mathsf{d}_K=0}\} = \frac{\lambda_{\text{ISI}}^m \, e^{-\lambda_{\text{ISI}}}}{m!} \tag{18a}$$

$$\text{Prob}\{\mathsf{c}_{\text{tot}} = m|_{\mathsf{d}_K=1}\} = \frac{(\lambda_K + \lambda_{\text{ISI}})^m \, e^{-(\lambda_K+\lambda_{\text{ISI}})}}{m!} \,, \tag{18b}$$

where λ_K is obtained by (17) for $k = K$, while λ_{ISI} can be evaluated as the sum of the means of each term in (16), as follows:

$$\lambda_K = N_{\text{Tx}} F_{\text{hit}}(d, T_{\text{b}}) \tag{19a}$$

$$\begin{aligned}\lambda_{\text{ISI}} &= \sum_{k=0}^{K-1} \mathbb{E}\{\mathsf{d}_k\}\lambda_k \\ &= p_1 N_{\text{Tx}} \sum_{k=0}^{K-1} \overbrace{\overline{F}_{T_{\text{b}}}[d, (K-k)T_{\text{b}}]}^{=F_{\text{hit}}[d,(K-k+1)T_{\text{b}}]-F_{\text{hit}}[d,(K-k)T_{\text{b}}]} \\ &= p_1 N_{\text{Tx}}[F_{\text{hit}}(d, KT_{\text{b}}+T_{\text{b}}) - F_{\text{hit}}(d, T_{\text{b}})] \,.\end{aligned} \tag{19b}$$

We recall that, in case of no molecule degradation, $F_{\text{hit}}(d, t)$ in (19) is given by (1) while, with molecule degradation, it is provided by (6).

[9]The intensity function $\rho(t)$ of a generic time domain point process (PP) in [20] is going to be identified with $\lambda(t)$ in this case, since here we deal with a time domain PPP.

[10]Recall that if each point of a stationary PPP is deleted with probability p, the resulting point process is still Poisson with mean scaled by a factor of $1-p$ (see [55]).

[11]The sum of independent Poisson RVs is a Poisson RV with parameter equal to the sum of the parameters.

2) Data transmission with Poisson timing transmitter: In the case of Poisson timing transmitter, molecules emissions randomly occur one by one during the whole interval $[0, (K+1)T_{\mathrm{b}}]$. However, the statistical characterization of the random emission time instants τ_n belonging to the time domain PPP Π is based on a continuous-time function, that is the intensity function $\lambda_{\mathrm{Tx}}(t)$ of Π. Indeed, for the point processes theory [55]–[58], the probability that there is a point of Π in the interval $[t, t+dt]$ is $\lambda_{\mathrm{Tx}}(t)dt$. Furthermore, by denoting as $a(t)$ the propensity function of the chemical reaction that leads to the emission of molecules [13], the probability that an emission occurs in the interval $[t, t+dt]$ is equal to $a(t)dt$. Thus the intensity function of Π can be seen as the propensity function. In other words, in such a molecular emission model, data transmission is based on controlling $a(t)$ in the same way that, in traditional communications, it is based on controlling the waveform. We assume to control the emission of molecules over time (in terms of the probability of emission in a given interval) in such a way that:

$$\lambda_{\mathrm{Tx}}(t) = \sum_{k=0}^{K} \mathsf{d}_k \; g(t - kT_{\mathrm{b}}) \; , \tag{20}$$

where $g(t)$ can be considered a sort of waveform with duration (activation time) $T_{\mathrm{a}} \leqslant T_{\mathrm{b}}$ such that $\int_0^{T_{\mathrm{a}}} g(t)dt = N_{\mathrm{Tx}}$ and $g(t) = 0$ outside $[0, T_{\mathrm{a}}]$. According to (14), the number of molecules received in the interval $[KT_{\mathrm{b}},\, (K+1)T_{\mathrm{b}}]$ can be written as:

$$\mathsf{c}_{\mathrm{tot}} \sim \mathrm{Pois}\left(\lambda_{\mathrm{tot}}\right) \; , \tag{21}$$

where, by setting $t_0 = KT_{\mathrm{b}}$ and $T_0 = T_{\mathrm{b}}$, and using the properties of the Poisson RVs, we obtain

$$\begin{aligned}
\lambda_{\mathrm{tot}} &= \mathbb{E}\left\{\mathsf{a}[KT_{\mathrm{b}}, KT_{\mathrm{b}} + T_{\mathrm{b}}]\right\}_{\lambda_{\mathrm{Tx}}}^{(\mathrm{tim})} \\
&= \int_0^{+\infty} \mathbb{E}\left\{\lambda_{\mathrm{Tx}}(\tau)\right\} \overline{F}_{T_{\mathrm{b}}}(d, KT_{\mathrm{b}} - \tau)d\tau \\
&= \sum_{k=0}^{K} \mathbb{E}\left\{\mathsf{d}_k\right\} \int_0^{+\infty} g(\tau - kT_{\mathrm{b}}) \overline{F}_{T_{\mathrm{b}}}(d, KT_{\mathrm{b}} - \tau)d\tau \\
&= p_1 \sum_{k=0}^{K} \lambda_k \; ,
\end{aligned} \tag{22}$$

where the first equality follows by substituting (14) and taking the average given the fixed $\{\mathsf{d}_k\}$, the second equality is derived by averaging with respect to $\{\mathsf{d}_k\}$ and utilizing linearity, and the third equality is obtained by defining:

$$\begin{aligned}
\lambda_k &\triangleq \int_0^{+\infty} g(\tau - kT_{\mathrm{b}}) \overline{F}_{T_{\mathrm{b}}}(d, KT_{\mathrm{b}} - \tau)d\tau \\
&= \int_0^{T_{\mathrm{a}}} g(\tau) \overline{F}_{T_{\mathrm{b}}}[d, (K-k)T_{\mathrm{b}} - \tau]d\tau \, .
\end{aligned} \tag{23}$$

For a given value of d_K, (22) can be written as $\lambda_{\mathrm{tot}} = \mathsf{d}_K \lambda_K + p_1 \sum_{k=0}^{K-1} \lambda_k$. Thus, thanks to the properties of the Poisson RV,[12] $\mathsf{c}_{\mathrm{tot}}|_{\mathsf{d}_K}$ can be decomposed as:[13]

$$\mathsf{c}_{\mathrm{tot}}|_{\mathsf{d}_K} = \mathsf{d}_K \mathsf{c}_K + \mathsf{c}_{ISI} \sim \mathrm{Pois}\left(\mathsf{d}_K \lambda_K + p_1 \sum_{k=0}^{K-1} \lambda_k\right) \; , \tag{24}$$

where

$$\mathsf{c}_K \sim \mathrm{Pois}(\lambda_K) \tag{25}$$

$$\mathsf{c}_{ISI} \sim \mathrm{Pois}\left(\lambda_{\mathrm{ISI}}\right) \; , \tag{26}$$

with $\lambda_{\mathrm{ISI}} = p_1 \sum_{k=0}^{K-1} \lambda_k$. In other words, we can interpret $\mathsf{c}_{\mathrm{tot}}$ as the sum of the useful component and the ISI where both the components are Poisson RVs. From (23) we readily get

$$\lambda_K = \int_0^{T_{\mathrm{a}}} g(\tau) \overline{F}_{T_{\mathrm{b}}}[d, -\tau]d\tau = \int_0^{T_{\mathrm{a}}} g(\tau) F_{\mathrm{hit}}[d, T_{\mathrm{b}} - \tau]d\tau \tag{27a}$$

$$\begin{aligned}
\lambda_{\mathrm{ISI}} &= p_1 \sum_{k=0}^{K-1} \int_0^{T_{\mathrm{a}}} g(\tau) \overline{F}_{T_{\mathrm{b}}}[d, (K-k)T_{\mathrm{b}} - \tau]d\tau \\
&= p_1 \int_0^{T_{\mathrm{a}}} g(\tau) \overbrace{\sum_{k=0}^{K-1} \overline{F}_{T_{\mathrm{b}}}[d, (K-k)T_{\mathrm{b}} - \tau]}^{= F_{\mathrm{hit}}(d, KT_{\mathrm{b}} + T_{\mathrm{b}} - \tau) - F_{\mathrm{hit}}(d, T_{\mathrm{b}} - \tau)} d\tau \\
&= p_1 \left[\int_0^{T_{\mathrm{a}}} g(\tau) F_{\mathrm{hit}}(KT_{\mathrm{b}} + T_{\mathrm{b}} - \tau)d\tau \right. \\
&\quad \left. - \int_0^{T_{\mathrm{a}}} g(\tau) F_{\mathrm{hit}}(T_{\mathrm{b}} - \tau)d\tau \right] .
\end{aligned} \tag{27b}$$

Also in this case, therefore, the PMF of the total number of received molecules conditioned on d_K is formally expressed by (18), where now λ_K and λ_{ISI} are given by (27) instead of (19). Note that, for $g(t) = N_{\mathrm{Tx}}\delta(t)$, expressions (27) reduce to (19). For $g(t)$ equal to a rectangular pulse with amplitude $N_{\mathrm{Tx}}/T_{\mathrm{a}}$ and duration T_{a}, we can write, instead:

$$\lambda_{\mathrm{ISI}} = p_1 N_{\mathrm{Tx}} \left[F_{\mathrm{act}}(d, KT_{\mathrm{b}} + T_{\mathrm{b}}) - F_{\mathrm{act}}(d, T_{\mathrm{b}})\right] \tag{28a}$$

$$\lambda_K = N_{\mathrm{Tx}} F_{\mathrm{act}}(d, T_{\mathrm{b}}) \; , \tag{28b}$$

where the expression

$$F_{\mathrm{act}}(d, T) \triangleq \frac{1}{T_{\mathrm{a}}} \int_0^{T_{\mathrm{a}}} F_{\mathrm{hit}}(d, T - \tau)d\tau \tag{29}$$

depends on the eventual presence of molecule degradation.

[12]The sum of two independent Poisson RVs with parameters λ_K and λ_{ISI} is a Poisson RV with parameter $\lambda_K + \lambda_{\mathrm{ISI}}$. Conversely, a Poisson RV with parameter $\lambda_K + \lambda_{\mathrm{ISI}}$ can be seen as the sum of two independent Poisson RVs with parameters λ_K and λ_{ISI}.

[13]With a slight abuse of notation, we use $\mathsf{c}_{\mathrm{tot}}|_{\mathsf{d}_K}$ when we consider the PMF of the total number of received molecules conditioned to the value of the K-th data d_K, as in (24), while $\mathsf{c}_{\mathrm{tot}}$ when we consider the unconditional PMF, as in (21).

a) Without molecule degradation: In the case of no molecule degradation, (29) results in:

$$F_{\text{act}}(d,t) = \frac{1}{T_{\text{a}}}\int_0^{T_{\text{a}}} \frac{R}{d}\text{erfc}\left(\frac{d-R}{\sqrt{4D(T-\tau)}}\right)d\tau$$
$$= \frac{R}{d}\left\{\frac{T}{T_{\text{a}}}\text{erfc}\left(\frac{d-R}{2\sqrt{DT}}\right) - \left(\frac{T}{T_{\text{a}}}-1\right)\text{erfc}\left(\frac{d-R}{2\sqrt{D(T-T_{\text{a}})}}\right) - \frac{(d-R)^2\left[\Gamma\left(-\frac{1}{2},\frac{(d-R)^2}{4DT}\right)-\Gamma\left(-\frac{1}{2},\frac{(d-R)^2}{4D(T-T_{\text{a}})}\right)\right]}{4\sqrt{\pi}DT_{\text{a}}}\right\}, \quad (30)$$

where $\Gamma(s,x)$ is the upper incomplete Gamma function.

b) With molecule degradation: In case of molecule degradation, (29) becomes, after some algebra:

$$F_{\text{act}}(d,T) = \frac{R\,A(d)}{2d}\left[1-E^{(+)}_{T_{\text{a}}}(d,T)\right] + \frac{R}{2d\,A(d)}\left[1-E^{(-)}_{T_{\text{a}}}(d,T)\right], \quad (31)$$

where we defined

$$A(d) \triangleq e^{\sqrt{\frac{k_{\text{d}}}{D}}(d-R)} \quad (32a)$$

$$h(d) \triangleq \frac{4D}{(d-R)^2} \quad (32b)$$

$$E^{(+)}_{T_{\text{a}}}(d,T) \triangleq \frac{1}{T_{\text{a}}}\int_0^{T_{\text{a}}}\text{erf}\left(\frac{1}{\sqrt{h(d)(T-\tau)}}+\sqrt{k_{\text{d}}(T-\tau)}\right)d\tau \quad (32c)$$

$$E^{(-)}_{T_{\text{a}}}(d,T) \triangleq \frac{1}{T_{\text{a}}}\int_0^{T_{\text{a}}}\text{erf}\left(\frac{1}{\sqrt{h(d)(T-\tau)}}-\sqrt{k_{\text{d}}(T-\tau)}\right)d\tau\,, \quad (32d)$$

with the resulting expression of $E^{(+)}_{T_{\text{a}}}(d,T)$ and $E^{(-)}_{T_{\text{a}}}(d,T)$ reported in (57) and (58), respectively (see Appendix A).

B. Bit Error Probability

Let us denote the threshold as N_{th}. For both transmitter models, the BEP conditioned on having transmitted a 0 at the K-th instant is

$$P_{\text{e}}|_0 = \text{Prob}\{\mathsf{c}_{\text{tot}}|_{\mathsf{d}_K=0} > N_{\text{th}}\} = \text{Prob}\{\mathsf{c}_{ISI} > N_{\text{th}}\} = 1 - Q(\lfloor N_{\text{th}}+1\rfloor, \lambda_{\text{ISI}})\,, \quad (33)$$

where $Q(s,x)$ is the regularized upper incomplete Gamma function, defined as

$$Q(s,x) \triangleq \frac{1}{\Gamma(s)}\int_x^{+\infty} t^{s-1}e^{-t}dt\,, \quad (34)$$

with $\Gamma(\cdot)$ being the ordinary gamma function.

The BEP conditioned to having transmitted a 1 at the K-th instant is

$$P_{\text{e}}|_1 = \text{Prob}\{\mathsf{c}_{\text{tot}}|_{\mathsf{d}_K=1} < N_{\text{th}}\} = \text{Prob}\{\mathsf{c}_K + \mathsf{c}_{ISI} < N_{\text{th}}\} = Q(\lfloor N_{\text{th}}+1\rfloor, \lambda_K+\lambda_{\text{ISI}})\,, \quad (35)$$

where λ_K and λ_{ISI} are provided by (19) and (27) for the Poisson concentration and timing transmitter models, respectively. The unconditioned BEP can be computed as:

$$P_{\text{e}} = p_0 P_{\text{e}}|_0 + p_1 P_{\text{e}}|_1\,, \quad (36)$$

which depends on the chosen threshold N_{th} via (33) and (35). However, once λ_{ISI} and λ_K are known, the discrete threshold value minimizing (36) can be obtained as suggested by [18]. Given the discrete nature of such an optimization problem, we can evaluate (36) among all possible options $[0, \lambda_K+\lambda_{\text{ISI}}]$ and then choose

$$N^*_{\text{th}} \triangleq \arg\min_{N_{\text{th}}} P_{\text{e}}\,. \quad (37)$$

All of the results that are further discussed assume the choice $N_{\text{th}} = N^*_{\text{th}}$.

IV. Sensing functionality

We define the sensing functionality in terms of the localization of the molecule emitter. In this section, we introduce the concept of Fisher information applied to molecular localization to derive the CRB on the error in position estimation. The rationale lies in the possibility of obtaining lower bounds on performance curves that are absolutely general, meaning they do not depend on the specific estimation algorithm used (assuming it is based on the observation of received molecules).[14]. We revisit the methodology presented in [49] for the formal setup of the problem. However, starting from the calculation of the log-likelihood function, we need to develop a new framework based on the Poisson statistics of the received molecules (inherently different, as it is discrete, from the continuous Gaussian statistics typically involved in traditional localization).

A. Cooperative localization

We denote as $\boldsymbol{p} \triangleq [x,y,z]^T$ the unknown 3D position of the target (the nanomachine working as transmitter) which is to be estimated, and as $\boldsymbol{p}_l \triangleq [x_l,y_l,z_l]^T$ the known 3D coordinates of the l-th receiver working as anchor. Let $L \geqslant 4$ the number of receivers/anchors. The distance between the target and the l-th anchor is

$$d_l = \|\boldsymbol{p}-\boldsymbol{p}_l\| = \sqrt{(x_l-x)^2+(y_l-y)^2+(z_l-z)^2}\,. \quad (38)$$

The range measurement is done based on the observation r_l of the number of molecules received by the l-th anchor in the interval $[0,T_0]$, where we can consider $T_0 = (K+1)T_{\text{b}}$ as a reference, due to the emission at all bit time $\{kT_{\text{b}}\}$. Based on the previous discussion, r_l can be modeled as a Poisson RV with parameter λ_l depending on the transmitter model.

Let us define the observations vector $\mathbf{r}$ as

$$\mathbf{r} \triangleq [r_1, r_2, \ldots, r_L]^T\,. \quad (39)$$

[14]As is well known, the CRB, based on the performance of a hypothetical maximum likelihood (ML) estimator, provides a theoretical minimum bound on the variance of the error, which in reality will always be greater than (or at most equal to) that of the ML estimator (for which, moreover, an explicit derivation is not required for the purposes of the CRB)

By considering the L receivers far enough to neglect the correlation between the observations r_l the case of absorbing receivers, we can write the PMF of $\mathbf{r}$ as:

$$p(\mathbf{r}) \triangleq \text{Prob}\{r_1 = n_1, r_2 = n_2, \ldots, r_L = n_L\} = \prod_{l=1}^{L} \text{Prob}\{r_l = n_l\} = \prod_{l=1}^{L} \frac{\lambda_l^{n_l}\, e^{-\lambda_l}}{n_l!}\,. \tag{40}$$

The log-likelihood of the observations is:

$$\ln p(\mathbf{r}) = \ln\left[\prod_{l=1}^{L} \frac{\lambda_l^{n_l}\, e^{-\lambda_l}}{n_l!}\right] = \sum_{l=1}^{L} \ln\left(\frac{\lambda_l^{n_l}\, e^{-\lambda_l}}{n_l!}\right) = \sum_{l=1}^{L} \left[\ln\left(\frac{\lambda_l^{n_l}}{n_l!}\right) - \lambda_l\right] = \sum_{l=1}^{L} \left[n_l \ln \lambda_l - \lambda_l - \ln n_l!\right]\,. \tag{41}$$

As is known, the Fisher information matrix (FIM) is calculated by taking the second derivatives of the log-likelihood function with respect to the components of the parameter vector to be estimated (in this case, the position vector $\boldsymbol{p}$). Thus, a 3×3 matrix, denoted as $[\mathbf{J}(\boldsymbol{p})]_{3\times 3}$, will be obtained, whose elements can be derived starting from (41). In the Appendix B we show that $\mathbf{J}(\boldsymbol{p})_{3\times 3}$ results in (67), where the expression for λ_l (the parameter of the l-th observation r_l) depends on the transmitter model and will be evaluated in the following subsections. Therefore, denoting $\hat{\boldsymbol{p}}$ as the estimated position of the target, the Cramér-Rao Bound on the localization error results in:

$$\mathbb{E}\left\{\|\hat{\boldsymbol{p}} - \boldsymbol{p}\|^2\right\} \geqslant \text{CRB}(\boldsymbol{p}) \;\triangleq\; \text{Tr}\left\{[\mathbf{J}^{-1}(\boldsymbol{p})]_{3\times 3}\right\}\,. \tag{42}$$

B. Localization with Poisson concentration transmitter

For the case of Poisson concentration transmitter, using (10) with $T_0 = (K+1)T_\text{b}$, $t_0 = 0$, and $\tau_0 = kT_\text{b}$, considering the superposition effects and the properties of the Poisson RVs, the observation variable r_l has parameter[15]

$$\lambda_l = \mathbb{E}\left\{\mathsf{a}[0, T_0]_{kT_\text{b}}^{(\text{con})}\right\} = p_1 N_\text{Tx} \sum_{k=0}^{K} \overline{F}_{T_0}(d_l, -kT_\text{b}) = p_1 N_\text{Tx} \sum_{k=0}^{K} F_\text{hit}(d_l, T_0 - kT_\text{b})\,, \tag{43}$$

where the last equalities follow from the fact that $F_\text{hit}(d,t)$ is identically zero for $t \leqslant 0$. Thus, we have

$$\frac{\partial \lambda_l}{\partial x} = p_1 N_\text{Tx} \sum_{k=0}^{K} \frac{\partial F_\text{hit}(d_l, T_0 - kT_\text{b})}{\partial d_l} \frac{\partial d_l}{\partial x}\,, \tag{44}$$

where, from (38) it is:

$$\frac{\partial d_l}{\partial x} = \frac{2(x_l - x)(-1)}{2\sqrt{(x_l - x)^2 + (y_l - y)^2 + (z_l - z)^2}}\,. \tag{45}$$

and (as for the BEP evaluation) the expression of $F_\text{hit}(d,t)$ to be used depends on the possible degradation of the molecules.

1) FIM coefficients without molecule degradation: In the case of no molecule degradation, we use (1) in (43) to find λ_l. Then we derive (1) with respect d, yielding:

$$\frac{\partial F_\text{hit}(d,t)}{\partial d} = -\frac{R}{d^2}\text{erfc}\left(\frac{d-R}{\sqrt{4Dt}}\right) - \frac{R}{d\sqrt{\pi D t}} e^{-\frac{(d-R)^2}{4Dt}}\,. \tag{46}$$

By using (46) in (44) we can calculate $\frac{\partial \lambda_l}{\partial x}$ and thus the $(1,1)$ element of the FIM. All other elements of the FIM can be obtained by doing the same for the remaining coordinates y and z, using the results in accordance with (67).

2) FIM coefficients with molecule degradation: In the case of molecule degradation, we need to incorporate (6) in (43) to get λ_l. Next, we derive (6) with respect d, obtaining:[16]

$$\begin{aligned}\frac{\partial F_\text{hit}(d,t)}{\partial d} =& -\frac{R}{2d}\frac{\left(\frac{1}{d} - \sqrt{\frac{k_\text{d}}{D}}\right)}{e^{-\sqrt{\frac{k_\text{d}}{D}}(d-R)}}\text{erfc}\left(\frac{d-R}{\sqrt{4Dt}} + \sqrt{k_\text{d} t}\right) \\ &- \frac{R}{2d}\frac{\left(\frac{1}{d} + \sqrt{\frac{k_\text{d}}{D}}\right)}{e^{\sqrt{\frac{k_\text{d}}{D}}(d-R)}}\text{erfc}\left(\frac{d-R}{\sqrt{4Dt}} - \sqrt{k_\text{d} t}\right) \\ &- \frac{R}{2d}\frac{e^{\sqrt{\frac{k_\text{d}}{D}}(d-R)}}{\sqrt{\pi D t}} e^{-\left(\frac{d-R}{\sqrt{4Dt}} + \sqrt{k_\text{d} t}\right)^2} \\ &- \frac{R}{2d}\frac{e^{-\sqrt{\frac{k_\text{d}}{D}}(d-R)}}{\sqrt{\pi D t}} e^{-\left(\frac{d-R}{\sqrt{4Dt}} - \sqrt{k_\text{d} t}\right)^2}\,.\end{aligned} \tag{47}$$

By using (47) in (44) we get $\frac{\partial \lambda_l}{\partial x}$ and thus the element $(1,1)$ of the FIM. All other elements can be derived by doing the same for the remaining coordinates y and z, utilizing the results in accordance with (67).

C. Localization with Poisson timing transmitter

For the case of Poisson timing transmitter, by using (14) with $t_0 = 0$ and the properties of the Poisson RVs, we can show that r_l has parameter[17]

$$\begin{aligned}\lambda_l &= p_1 \sum_{k=0}^{K} \int_0^{+\infty} g(\tau - kT_\text{b}) \overline{F}_{T_0}(d_l, -\tau) d\tau \\ &= p_1 \sum_{k=0}^{K} \int_0^{T_\text{a}} g(\tau) F_\text{hit}(d_l, T_0 - kT_\text{b} - \tau) d\tau\,.\end{aligned} \tag{48}$$

Thus, we have

$$\frac{\partial \lambda_l}{\partial x} = p_1 \sum_{k=0}^{K} \int_0^{T_\text{a}} g(\tau) \frac{\partial F_\text{hit}[d_l, T_0 - kT_\text{b} - \tau]}{\partial d_l} \frac{\partial d_l}{\partial x} d\tau\,, \tag{49}$$

where $\frac{\partial F_\text{hit}(d,t)}{\partial d}$ and $\frac{\partial d_l}{\partial x}$ are provided by (47) and (45), respectively. It can be noted that, as expected, for $g(t) = N_\text{Tx}\delta(t)$, (48) reduces to (43) and (49) to (44) (the timing transmitter reduces to te concentration transmitter for $T_\text{a} \to 0$).

[15] Easily apply the same steps used to derive the first equality in (19) with the summation extended from $K-1$ to K (because even molecules bound to the K-th data contribute to the estimate) and with $\overline{F}_{T_\text{b}}(d,\cdot)$ replaced by $\overline{F}_{T_0}(d_l,\cdot)$, because now the observation interval extends from $t_0 = 0$ to $T_0 = (K+1)T_\text{b}$, not just the K-th bit time, and the distance refers to the l-receiver.

[16] As a sanity check, it can be recognized that (47) reduced to (46) for $k_\text{d} = 0$.

[17] It is sufficient to use the same methodology adopted for the derivation of (22) with $\overline{F}_{T_0}(d_l,\cdot)$ in place of $\overline{F}_{T_\text{b}}(d,\cdot)$.

If, instead, $g(t)$ is a rectangular pulse with duration $T_{\rm a} \leqslant T_{\rm b}$ and amplitude $N_{\rm Tx}/T_{\rm a}$ we get:

$$\lambda_l = p_1 N_{\rm Tx} \sum_{k=0}^{K} \frac{1}{T_{\rm a}} \int_0^{T_{\rm a}} F_{\rm hit}(d_l, T_0 - kT_{\rm b} - \tau) d\tau$$
$$= p_1 N_{\rm Tx} \sum_{k=0}^{K} F_{\rm act}(d_l, T_0 - kT_{\rm b}) \quad (50)$$

and

$$\frac{\partial \lambda_l}{\partial x} = p_1 \sum_{k=0}^{K} f_{\rm act}(d_l, T_0 - kT_{\rm b}) \frac{\partial d_l}{\partial x} \,, \quad (51)$$

where

$$f_{\rm act}(d, T) \triangleq \frac{1}{T_{\rm a}} \int_0^{T_{\rm a}} \frac{\partial F_{\rm hit}(d, T-\tau)}{\partial d} d\tau \,, \quad (52)$$

$\frac{\partial d_l}{\partial x}$ is given by (45), and the expression of $F_{\rm act}(d,T)$ and $F_{\rm hit}(d,T)$ to be used depend on the eventual presence of the molecule degradation.

1) FIM coefficients without molecule degradation: In the absence of molecular degradation, we use (30) in (50) to determine λ_l and (46) in (52) to get $f_{\rm act}(d,T)$. Thus, we obtain:

$$f_{\rm act}(d,T) = -\frac{R}{d^2}\Bigg\{\frac{T}{T_{\rm a}}\text{erfc}\left(\frac{d-R}{2\sqrt{DT}}\right) - \left(\frac{T}{T_{\rm a}}-1\right)\text{erfc}\left(\frac{d-R}{2\sqrt{D(T-T_{\rm a})}}\right) - \frac{(d-R)^2\left[\Gamma\left(-\frac{1}{2},\frac{(d-R)^2}{4DT}\right)-\Gamma\left(-\frac{1}{2},\frac{(d-R)^2}{4D(T-T_{\rm a})}\right)\right]}{4\sqrt{\pi}DT_{\rm a}}\Bigg\} + \frac{R}{d}\frac{\sqrt{T-T_{\rm a}}E_{\frac{3}{2}}\left(\frac{(d-R)^2}{4D(T-T_{\rm a})}\right)-\sqrt{T}E_{\frac{3}{2}}\left(\frac{(d-R)^2}{4DT}\right)}{\sqrt{\pi D}\,T_{\rm a}} \,, \quad (53)$$

where

$$E_a(x) \triangleq \int_1^{+\infty} e^{-xt} t^a dt \quad (54)$$

is the generalized exponential integral function. By substituting (53) in (51), $\frac{\partial \lambda_l}{\partial x}$ is obtained, as well as the element $(1,1)$ of the FIM. The other elements can be derived similarly for coordinates y and z, using the results in accordance with (67), as in the previous case.

2) FIM coefficients with molecule degradation: In the case of molecule degradation, we use (31) in (50) to calculate λ_l and (47) in (52) to find $f_{\rm act}(d,T)$. After some algebra, we obtain:

$$f_{\rm act}(d,T) = -\frac{R}{2d}\Bigg\{A(d)\left(\frac{1}{d}-\sqrt{\frac{k_{\rm d}}{D}}\right)\left[1-E^{(+)}_{T_{\rm a}}(d,T)\right] + \frac{\left(\frac{1}{d}+\sqrt{\frac{k_{\rm d}}{D}}\right)}{A(d)}\left[1-E^{(-)}_{T_{\rm a}}(d,T)\right] + G(d,T)\Bigg\} \,, \quad (55)$$

where $G(d,T)$ is defined by (56). By using(55) in (51) we obtain $\frac{\partial \lambda_l}{\partial x}$ and thus the element $(1,1)$ of the FIM. The other elements can be obtained according to (67) by performing similar operations for the coordinates y and z.

V. Numerical Results

In this section, we derive numerical results from the analytical framework, both in cases with and without molecule degradation.

A. Parameters values

Unless otherwise specified, the adopted parameters values are those indicated in Tab. I and justified as follows. Concerning the radius of each fully absorbing receiver, we adopt $R = 5\mu$m as considered in the initial study on the impact of multiple receivers [59]. Results are presented in a case study comprising a scenario with $L = 8$ spherical receivers positioned at the vertices of a cube with side length $l_{\rm Rx} = 50\mu$m. For simplicity, the target position is assumed at the center of the cube. In this configuration, the distance between the target and each receiver is $d_l = d = 2l_{\rm Rx} = 100\mu$m for all l making it irrelevant which receivers is chosen for evaluating communication performance. Note that we have chosen the distance values of our geometric setup such that the minimum distance between each receiver is always almost approximately one order of magnitude greater than the spherical receiver's radius R, thus allowing neglect of impairment effects studied in [59].

For the parameters related to molecular communication, the diffusion coefficient is set to $D = 1000\mu\text{m}^2/s$, based on foundational work on diffusion-based molecular channel capacity [11]. The average number of transmitted molecules, $N_{\rm Tx} = 10^4$, is the middle value (on a logarithmic scale) from the range $[10^3 - 10^5]$, studied in [18], where molecular degradation reduces ISI. Additionally, we choose the maximum degradation rate of molecules such that half-life matches the bit time (set to $T_{\rm b} = 0.25$s in our case), i.e., $k_{\rm d} = \ln(2)/T_{\rm b} \approx 0.277\ \text{s}^{-1}$. The resulting range for $k_{\rm d}$, as well as the value chosen for $T_{\rm b}$, fall within the respective intervals considered in [18].

Activation times ($T_{\rm a} = 25ms,\ 125ms,\ 225ms$) represent short, medium, and long durations relative to the bit time, corresponding to $1/10$, $1/2$, and $9/10$ of $T_{\rm b}$, respectively. Regarding the number of transmitted symbols (related to ISI length), we consider two cases. Without molecular degradation, we choose values ($K = 0,\ 2,\ 4,\ 8$) due to their known negative impact on BEP. However, in the presence of molecular degradation, these values can increase exponentially without affecting BEP, so we select powers of the maximum value from the previous range ($K = 8,\ 8^2,\ 8^3$).

B. The effect of the number of transmitted molecules

The expression of the BEP as a function of the number of molecules with and without molecular degradation has already been studied in [18], assuming concentration transmitter: here we additionally consider of the case of timing transmitter. Additionally, it is interesting to compare the performance in

$$G(d,T) \triangleq \frac{1}{\sqrt{Dk_{\rm d}}T_{\rm a}}\left\{\frac{1}{A(d)}\left[\text{erf}\left(\frac{1}{\sqrt{h(d)(T-T_{\rm a})}}-\sqrt{k_{\rm d}(T-T_{\rm a})}\right)-\text{erf}\left(\frac{1}{\sqrt{h(d)T}}-\sqrt{k_{\rm d}T}\right)\right]\right.$$
$$\left.+A(d)\left[\text{erf}\left(\frac{1}{\sqrt{h(d)T}}+\sqrt{k_{\rm d}T}\right)-\text{erf}\left(\frac{1}{\sqrt{h(d)(T-T_{\rm a})}}+\sqrt{k_{\rm d}(T-T_{\rm a})}\right)\right]\right\} \quad (56)$$

TABLE I
RANGE OF PARAMETERS ADOPTED IN NUMERICAL RESULTS

Parameter	Values
Average number of transmitted molecules ($N_{\rm Tx}$)	10^4 (see [18])
Diffusion coefficient (D)	1000 μm^2/s (see [11])
Radius of the receivers (R)	5 μm (see [59])
Molecule degradation rate ($k_{\rm d}$)	$[0-0.277]$ s^{-1}
Number of receivers (L)	8
Minimum distance between Rxs ($l_{\rm Rx}$)	50 μm
Tx - Rx distance (d)	100 μm
Probability to transmit '0' (p_0)	0.5
and "1" (p_1)	0.5
Number of transmitted symbols (K)	$\{0,2,4,8\}$, $\{0,8,64,512\}$
Bit time ($T_{\rm b}$)	0.25 s
Activation time ($T_{\rm a}$)	$\{25,125,225\}$ ms

terms of communication with that in terms of localization with an equal number of received molecules, to determine which of the two tasks is more demanding, once threshold values are fixed for both functionalities.

In Fig. 3(a) the BEP is depicted as a function of the average number of transmitted molecules $N_{\rm Tx}$ for different values of transmitted symbols, in a scenario with no molecule degradation. Both concentration and timing Poisson transmitter models are considered. As expected, the BEP is a decreasing function of $N_{\rm Tx}$, but the impact of the ISI is dramatic in this scenario. Indeed, we can observe that, with no ISI ($K=0$) the BEP drops under 10^{-3} for less than $2\cdot10^3$ transmitted molecules (in the case of Poisson concentration transmitter) while, with just two interfering symbols even $2\cdot10^4$ molecules are insufficient to have the same low BEP. With $K=4$ and $K=8$ interfering symbols, the BEP results in approximately 10^{-2} and 0.05, respectively, for $N_{\rm Tx}=2\cdot10^4$. In the case of Poisson timing transmitter (with activation time $T_{\rm a}=T_{\rm b}/2=0.125$ s), BEP values increase (for each value of K) by about one order of magnitude for the same number of transmitted molecules $N_{\rm Tx}$. This is because in the timing model, molecules can be transmitted with a delay of $T_{\rm a}$ relative to the start of the bit time (and observation time), resulting in a lower average quantity of molecules received within the same observation time.

In Fig. 3(b) the same situation is analyzed in the presence of molecule degradation (with $k_d=\ln 2/T_{\rm b}\approx 0.277$ s).[18]. As expected, molecule degradation worsen the single BEP, but also reduces the impact of ISI in case of multiple symbols transmission. On the one hand, in the absence of ISI ($K=0$), more than $2\cdot10^3$ molecules are now needed to achieve a BEP below 10^{-3}. On the other hand, in the presence of ISI, (e.g., $K=8$), the BEP corresponding to $N_{\rm Tx}=2\cdot10^4$ decreases from about 0.05 to about 0.005 and remains the same also for higher number of transmitted symbols (e.g., $K=64,\ 512$). It is interesting to note that even in this scenario the impact of considering a Poisson timing (instead of concentration) transmitter (with a quite long activation time) is dramatic (the BEP for $N_{\rm Tx}=2\cdot10^4$ increases to 0.1).

In Fig. 3(c), we depict the trend of the normalized root CRB as a function of the average number of emitted molecules in the absence of molecular degradation for various values of K, in a scenario with no molecule degradation. Both concentration and timing Poisson transmitter models are again under investigation. As expected, the normalized root CRB decreases with an increase in the number of transmitted molecules, but unlike the BEP, it becomes lower with the growth of the ISI, which in this case has a constructive effect (symbols previously transmitted, representing interference on the communication side, reinforce the estimation SNR on the localization side). E.g., in case if no ISI ($K=0$), the normalized root CRB decreases from about 0.1 for $N_{\rm Tx}=10^3$ to about 0.02 for $N_{\rm Tx}=2\cdot10^4$, while, with $K=2,\ 4\ 8$, considering the same values for $N_{\rm Tx}$ as references, it decreases from about 0.05, 0.04, and 0.03 to about 0.01, 0.0085, and 0.0075, respectively. In this scenario, considering a Poisson timing instead of concentration transmitter model has ho dramatic effect on the localization as for the communication. Indeed, the curves are almost completely overlapping. Only in the no ISI case, a slight increase in the root CRB is noticeable. This can be explained by the fact that over an observation time span equal to $KT_{\rm b}$, the maximum delay of $T_{\rm a}$ in the emission of molecules becomes irrelevant (unlike in the communication case).

In Fig. 3(d) the same situation as Fig. 3(c) is analyzed in the presence of molecule degradation. As expected, molecular degradation diminishes the accuracy of the estimation upon which localization is based under the same conditions. Indeed, both for $K=0$ (black line) and $K=8$ (blue line), the normalized root CRB slightly increases (compared to the corresponding curves in the previous figure). However, since molecular degradation allows for the transmission of more symbols before ISI becomes detrimental, these symbols, as mentioned, tend to improve the estimation. Consequently, overall, much lower CRB values are observed for $K=64$ and $K=512$ compared to the previous cases. This can be easily explained: on one hand, molecule degradation reduces the number of molecules reaching the receiver after a certain time, thus reducing the effectiveness of estimation (which is based on the observation of the number of molecules received at instant $KT_{\rm b}$). On the other hand, by significantly

[18]This means that the half life of molecule equals the bit time

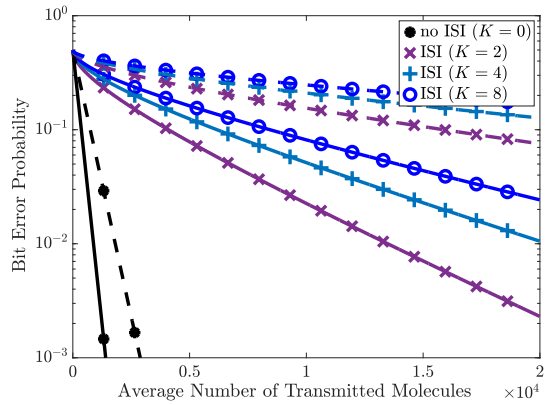

(a) BEP as a function of the average number of transmitted molecules without molecule degradation ($k_{\mathrm{d}} = 0$)

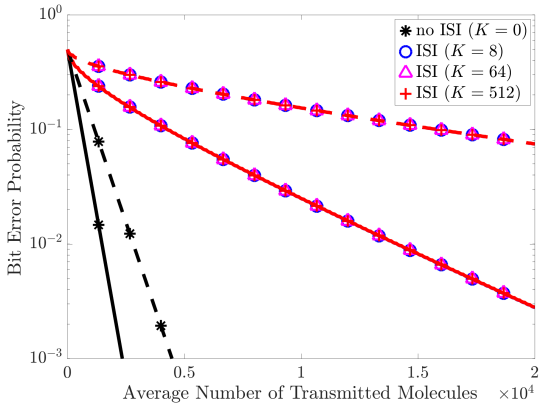

(b) BEP as a function of the average number of transmitted molecules with molecule degradation ($k_{\mathrm{d}} = \ln 2/0.25\ \mathrm{s}^{-1}$)

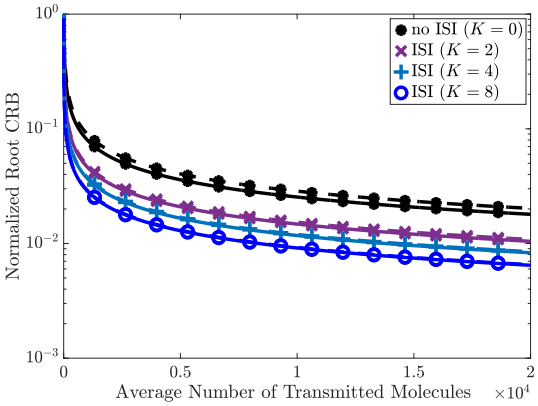

(c) Normalized Root CRB as a function of the average number of transmitted molecules N_{Tx} without molecule degradation ($k_{\mathrm{d}} = 0$)

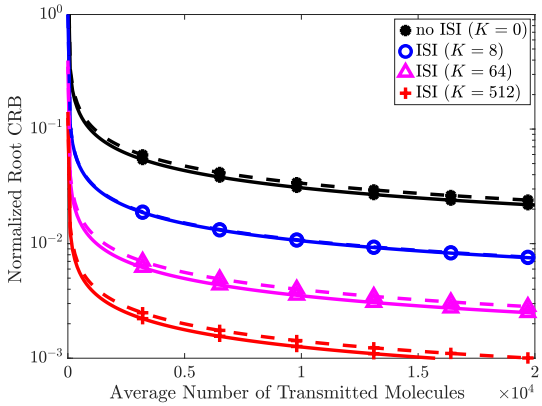

(d) Normalized Root CRB as a function of the average number of transmitted molecules N_{Tx} with molecule degradation ($k_{\mathrm{d}} = \ln 2/0.25\ \mathrm{s}^{-1}$)

Fig. 3. BEP and Normalized Root CRB as functions of the average number of transmitted molecules N_{Tx}. The continuous lines refer to the case of concentration transmitter, while the dashed lines to the case of transmitter timing model.

increasing K, the number of received molecules also increases, compensating greatly for degradation. Regardless of the presence or absence of molecular degradation, we can observe that considering a timing Poisson transmitter instead of a concentration one only slightly worsens the localization performance (in contrast to what happens for communication). This can be easily explained once again by considering that the maximum transmission delay of molecules in the case of a timing transmitter with activation time T_{a} becomes irrelevant compared to the observation time KT_{b} used in the localization task.

Looking at the four figures as a whole, we observe that, by targeting a BEP of 10^{-2} for communication performance and a normalized root CRB of 0.01 for localization performance, approximately 10^4 transmitted molecules are required on average for $K = 4$ in a scenario without molecule degradation. However, if the number of transmitted symbols increases or a timing transmitter used instead of a concentration model, the communication task becomes much more demanding in the terms of N_{Tx}. Conversely, the localization task requires only a slightly higher average number of transmitted molecules.

In the case of molecule degradation (again targeting a BEP of 10^{-2} and a normalized root CRB of 0.01 as targets), when $K = 8$, approximately $12 \cdot 10^3$ transmitted molecules are required for both communication and localization tasks. However, as K increases, the average number transmitted molecules required remains the same for the communication tasks, whereas the value of N_{Tx} required for the localization task can be significantly reduced with increasing K (e.g., N_{Tx} is in the order of thousands for $K = 64$ and in the order of hundreds for $K = 512$).

C. The effect of the distance

The performance, both in terms of communication reliability and localization precision, naturally deteriorates with increasing distance. However, it is interesting to compare the behavior of BEP with that of the CRB as a function of distance to ascertain whether, with threshold values set for both, the communication range exceeds or falls short of the localization range. In other words, whether molecular communications via diffusion are inherently more suited to one function over the other.

In Fig. 4(a), the BEP is depicted as a function of the distance in the no molecule degradation scenario. Both Poisson concen-

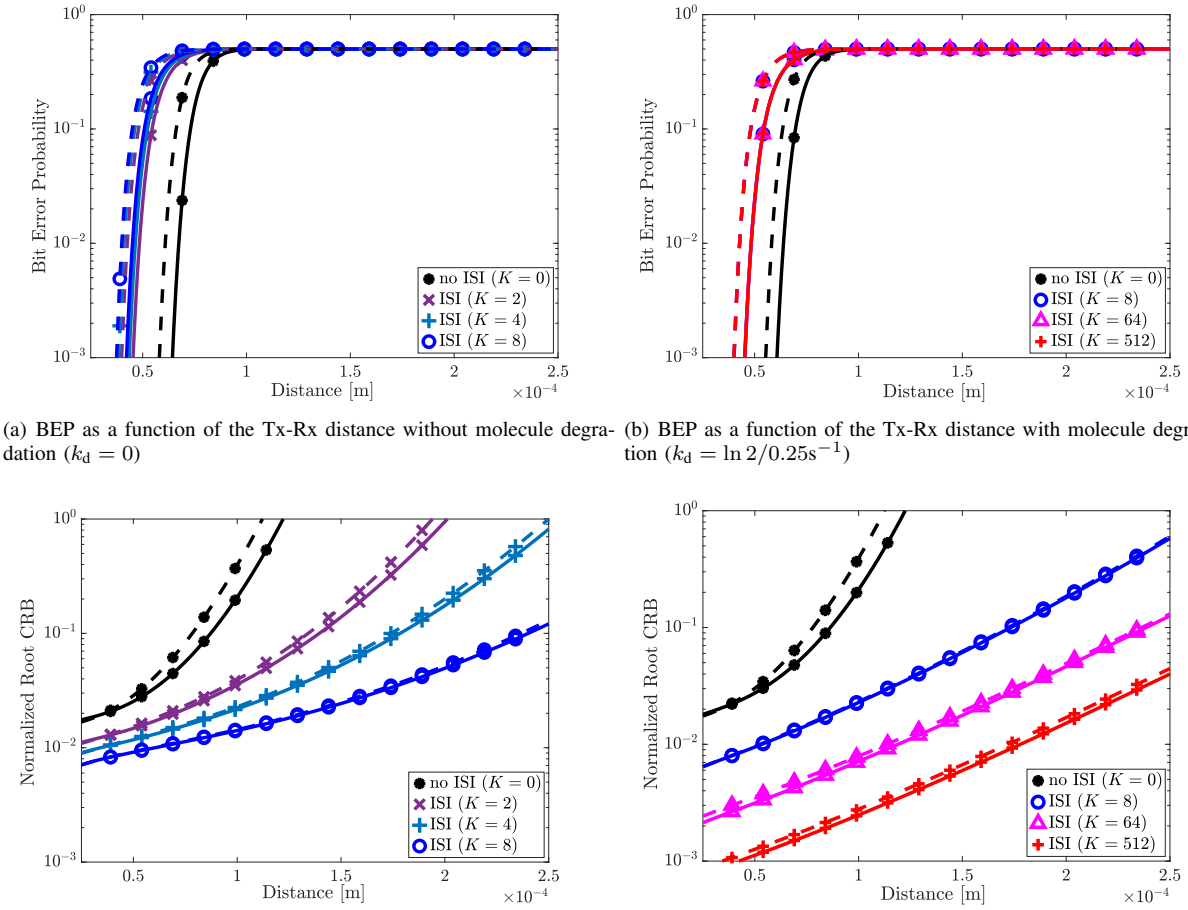

(a) BEP as a function of the Tx-Rx distance without molecule degradation ($k_\mathrm{d} = 0$)

(b) BEP as a function of the Tx-Rx distance with molecule degradation ($k_\mathrm{d} = \ln 2/0.25\mathrm{s}^{-1}$)

(c) Normalized Root CRB as a function of the Tx-Rx distance without molecule degradation ($k_\mathrm{d} = 0$)

(d) Normalized Root CRB as a function of the Tx-Rx distance with molecule degradation ($k_\mathrm{d} = \ln 2/0.25\mathrm{s}^{-1}$)

Fig. 4. BEP and Normalized Root CRB as functions of the Tx-Rx distance. The continuous lines refer to the case of concentration transmitter, while the dashed lines to the case of transmitter timing model.

tration and Poisson timing transmitted models are investigated. By considering a required BEP of 10^{-2}, we observe that, as expected, the communication range decreases in the presence of ISI (e.g., from more than about $60 - 70$ μm to values less than 50 μm, depending on K) as well as in the case of timing transmitter with activation $T_\mathrm{a} = T_\mathrm{b}/2$ (of about dozens of micrometers in all the cases).

In Fig. 4(b), the BEP is still depicted as a function of the distance, but in a scenario with molecule degradation (with $k_\mathrm{d} = \ln(2)/T_\mathrm{b}$). It is immediate to notice that the communication range slightly decrease (slightly more than 50 μm), with respect to the previous case, for no-ISI situation, while remains substantially the same as before (slightly less than 50 μm) for any positive value of K. Even in this case considering a Poisson timing transmitter model instead of a Poisson concentration on slightly reduce the corresponding communication performance. The motivations are the same just explained commenting Fig. 3.

In Fig. 4(c), the normalized root CRB is depicted as a function of distance in no molecule degradation scenario. Both Poisson concentration and Poisson timing transmitted models are investigated as before. By considering a required normalized root CRB of 10^{-2}, we observe that, for $K = 8$, the localization range is slightly higher than 50 μm.

In Fig. 4(b), the normalized root CRB is still depicted as a function of distance, but in a scenario with molecule degradation. In this scenario, with the required normalized root CRB always set to 10^{-2}, we observe that, for $K = 8$, the localization range is still slightly higher than 50 μm, while it increases to about 125 μm and 200 μm for $K = 64$ and $K = 512$, respectively. Even for what concerns the localization task the performance slightly decrease when a Poisson timing transmitter model is adopted instead of the Poisson concentration one.

Looking at the four figures collectively, we can observe that, while the communication range remains around 50 μm in all cases, the localization range can be expanded as desired by increasing the number of transmitted symbols. Naturally, this comes at the cost of increased waiting time to obtain the estimate, equivalent to KT_b.

D. JCS tradeoff without molecule degradation

If the increase in the average number of transmitted molecules improves both communication and localization performance, and increasing the distance worsens both, with an

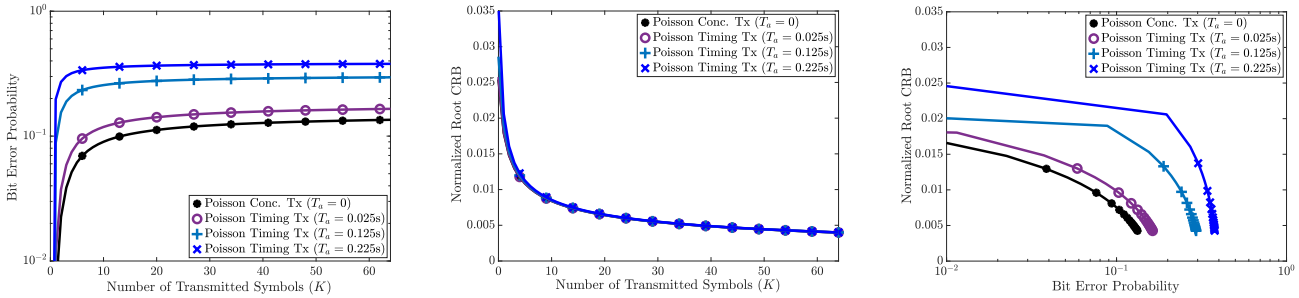

(a) BEP as a function of the number of transmitted symbols (K) without molecule degradation ($k_\mathrm{d} = 0$)

(b) Normalized Root CRB as a function of the number of transmitted symbols (K) without molecule degradation ($k_\mathrm{d} = 0$)

(c) Normalized Root CRB as a function of BEP without without molecule degradation ($k_\mathrm{d} = 0$)

Fig. 5. JCS tradeoff based on the number of transmitted symbols in absence of molecule degradation

.

increase in the number of transmitted symbols, the effect on the two tasks is instead opposite. Specifically, in the absence of molecular degradation, the effect of ISI is highly destructive for communication (because molecules emitted in previous symbol times also arrive in the observation window of the current symbol), while it is constructive for localization (since the position estimation is based on the number of molecules received within the estimation time window regardless of the bit time in which they were transmitted). Therefore, it makes sense (as in the case of traditional communications) to talk about seeking a tradeoff between communication and sensing. By adjusting the number of the transmitted symbols, we can move along on such a trade-off curve.

In Fig. 5(a) we depict the BEP as a function of transmitted symbols K for different values of the activation time T_a of the Poisson timing concentration transmitter ($T_\mathrm{a} = 0$ corresponds to Poisson concentration transmitter, while other values corresponds to $T_\mathrm{b}/10$, $T_\mathrm{b}/4$, and $0.9 \cdot T_\mathrm{b}$), in absence of molecule degradation. We notice that for K ranging from 0 to 64 the BEP raises from less than 10^{-2} to values in the interval $[0.1 - 0.4]$ depending on T_a. In Fig. 5(b), the normalized root CRB is represented as a function of K in the same scenario. We observe that, with K ranging from 0 to 64 as before, the normalized root CRB decreases from values in the interval $[0.025 - 0.035]$ (depending on T_a) to less than 0.005 (for all the considered values of T_a).

Given that both the expression of the BEP and the normalized root CRB are functions of K as shown, in Fig. 5(c) we depict the normalized root CRB as a function of the BEP, by varying K in the same range considered in the two previous figure, thus obtained the desiderd JCS tradeoff in absence of molecule degradation. We notice that for the case of Poisson concentration transmitter model, by accepting an increase of the BEP from 10^{-2} to 10^{-1}, the normalized root CRB can decrease from more than 0.015 to less than 0.001. In the case of Poisson timing transmitter, the value of the normalized root CRB decreases even more significantly as the activation time lengthens, for the same BEP.

E. JCS tradeoff with molecule degradation

In the case of molecular degradation, as ascertained in the preceding subsections, the impact of ISI on communication is reduced. Therefore, the tradeoff between communication and sensing needs to be sought by varying the degradation rate itself. On one hand, an increase in this coefficient reduces, as mentioned (and as shown in [18]), the number of received molecules emitted in the previous symbol intervals, thereby diminishing the impact of ISI and hence decreasing the BEP). On the other hand, high molecular degradation similarly reduces the number of molecules received in the entire observation interval KT_b used by localization, thus increasing the normalized root CRB.

In Fig. 6(a), we depict the BEP as a function of the molecule degradation rate k_d for different values of the activation time T_a of the Poisson timing concentration transmitter ($T_\mathrm{a} = 0$ corresponds to Poisson concentration transmitter), in the absence of molecular degradation. We notice that for k_d ranging from 0 to $\ln(2)/T_\mathrm{b}$, the BEP decreases from values around 10^{-1} (for $T_\mathrm{a} = 0.225$ s and $T_\mathrm{a} = 0.125$ s) and around 0.3 (for $T_\mathrm{a} = 0.025$s and $T_\mathrm{a} = 0$) to values around $3 \cdot 10^{-2}$ and around 0.2, respectively. In Fig. 6(b), the normalized root CRB is represented as a function of k_d in the same scenario. We observe that, for the same range of k_d, the normalized root CRB increases from values around 0.0092 to values in the interval $[0.0106 - 0.0109]$ (depending on T_a). The gap between lines referring to different values of T_a remains approximately the same in the considered range of k_d.

Now it is clear that, by adjusting the molecule degradation rate, we are able to move along the curve of JCS tradeoff. Fig 6(c) depicts the normalized root CRB as a function of the BEP and is obtained by varying k_d from 0 to $\ln(2)/T_\mathrm{b}$. We note that, in the case of Poisson concentration transmitter, by accepting an increase of the BEP from 0.03 to 0.08, the normalized root CRB decreases from 0.0106 to less than 0.0092. In the case of Poisson timing transmitter, the decrease of the normalized root CRB is more rapid the longer the activation time.

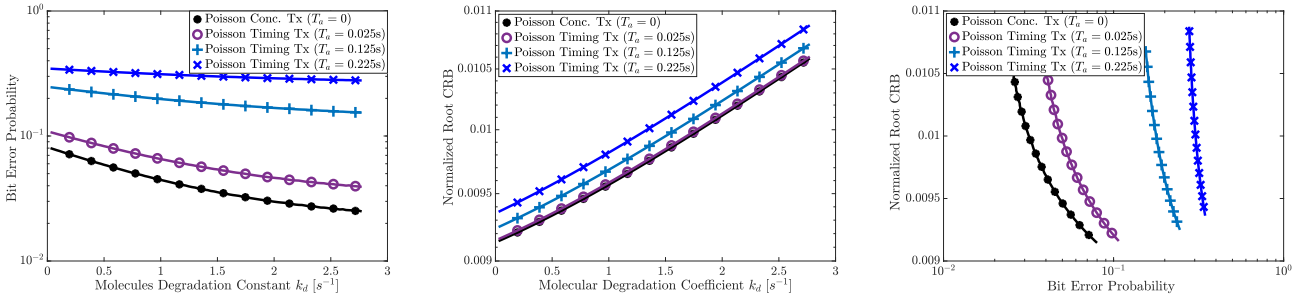

(a) BEP as a function of the molecule degradation rate k_{d} (b) Normalized Root CRB as a function of the molecule degradation rate k_{d} (c) Normalized Root CRB as a function of BEP

Fig. 6. JCS tradeoff based on the molecule degradation rate

.

F. Future Works

The future research directions in the field of molecular JCS could essentially be twofold in our view. On the communication side, one could explore the advantages of collaboration among different receivers (who already collaborate in localization in the proposed model), for example, by implementing soft decoding of the received symbols to reduce the probability of error. On the localization side, one could assess how much the performance of practically implementable algorithms deviates from the theoretical limits calculated in this work. We intend to pursue these directions in future works, as they go far beyond the scope of the present paper.

VI. Conclusion

In this paper a molecular JCS system where the communication function consists in transmitting information bits and the sensing function involves localizing the emitter is proposed and analyzed for the first time. More specifically, we propose a micro or nano scale dual function system where both the communication and the sensing tasks are based on molecules diffusion in an ideal fluid in three dimension. Under certain conditions, $L \geqslant 4$ fully absorbing spherical receivers are able to localize the position of a point wise target by counting the molecules that such a transmitter releases into the fluid to convey information to one of them. In such a scenario, we develop an analytical framework to investigate the fundamental limits in the terms of both communication and localization.

Closed form exact expressions for the BEP as well as for the CRB on the localization error are derived, for both Poisson concentration and timing transmitter models, with and without considering molecule degradation. Moreover, for the very fist time, theoretical trade-offs between communication and localization performance are established, with and without molecule degradation, by exploiting the simultaneous dependence of both the BEP and the CRB expressions on the number of the transmitted symbols and on the molecule degradation rate. In case of no molecule degradation, inter symbol interference has a strong negative impact on communication performance, while it has a costruttive effect on the localization. Thus, in such a case, the trade-off between communication and sensing can be obtained by varying the number of transmitted symbol. The introduction of molecule degradation improves the communication performance in the presence of ISI, while it reduces the effectiveness of the localization. Thus, in such a case, the trade-off between communication and sensing performance is obtained by varying the molecule degradation rate. Finally, we are able to compare communication and localization ranges, as well as the cost of both the functionalities in terms of average number of molecules that we need to emit to ensure given performance.

Appendix A
Auxiliary Functions

In this appendix, we report in (57) and (58) the expression for $E_{T_{\mathrm{a}}}^{(+)}(d,T)$ and $E_{T_{\mathrm{a}}}^{(-)}(d,T)$ obtained by calculating the integrals in their definitions (32c) and (32d).

Appendix B
Derivation of the Fisher Information Matrix

In this appendix we evaluate the FIM required for the calculation of the CRB on the localization error (42). The gradient of the log-likelihood (41) with respect to the position can be computed as:

$$\frac{\partial \ln p(\mathbf{r})}{\partial \boldsymbol{p}} \triangleq \left[\frac{\partial \ln p(\mathbf{r})}{\partial x}, \frac{\partial \ln p(\mathbf{r})}{\partial y}, \frac{\partial \ln p(\mathbf{r})}{\partial z}\right]^T, \tag{59}$$

where

$$\frac{\partial \ln p(\mathbf{r})}{\partial x} = \sum_{l=1}^{L}\left[\frac{n_l}{\lambda_l}\frac{\partial \lambda_l}{\partial x} - \frac{\partial \lambda_l}{\partial x}\right] = \sum_{l=1}^{L}\left(\frac{n_l}{\lambda_l} - 1\right)\frac{\partial \lambda_l}{\partial x} \tag{60a}$$

$$\frac{\partial \ln p(\mathbf{r})}{\partial y} = \sum_{l=1}^{L}\left[\frac{n_l}{\lambda_l}\frac{\partial \lambda_l}{\partial y} - \frac{\partial \lambda_l}{\partial y}\right] = \sum_{l=1}^{L}\left(\frac{n_l}{\lambda_l} - 1\right)\frac{\partial \lambda_l}{\partial y} \tag{60b}$$

$$\frac{\partial \ln p(\mathbf{r})}{\partial z} = \sum_{l=1}^{L}\left[\frac{n_l}{\lambda_l}\frac{\partial \lambda_l}{\partial z} - \frac{\partial \lambda_l}{\partial z}\right] = \sum_{l=1}^{L}\left(\frac{n_l}{\lambda_l} - 1\right)\frac{\partial \lambda_l}{\partial z}. \tag{60c}$$

$$E_{T_\mathrm{a}}^{(+)}(d,T) = \frac{1}{4\sqrt{\pi}k_\mathrm{d}h(d)T_\mathrm{a}}\Bigg[h(d)\exp\left(-\frac{k_\mathrm{d}h(d)(T^2+T_\mathrm{a}^2)+6T\sqrt{k_\mathrm{d}h(d)}+1}{h(d)(T-T_\mathrm{a})}\right)$$
$$\cdot\left(\sqrt{\pi}\,\mathrm{erf}\left(-\frac{\sqrt{k_\mathrm{d}h(d)}(T_\mathrm{a}-T)+1}{\sqrt{h(d)(T-T_\mathrm{a})}}\right)\exp\left(\frac{k_\mathrm{d}h(d)(T^2+T_\mathrm{a}^2)+2\sqrt{k_\mathrm{d}h(d)}(T+2T_\mathrm{a})+1}{h(d)(T-T_\mathrm{a})}\right)\right.$$
$$\left.+4\sqrt{k_\mathrm{d}T}\exp\left(\frac{k_\mathrm{d}h(d)TT_\mathrm{a}(T+T_\mathrm{a})+\sqrt{k_\mathrm{d}h(d)}2T(2T+T_\mathrm{a})+T_\mathrm{a}}{h(d)T(T-T_\mathrm{a})}\right)-4\sqrt{k_\mathrm{d}(T-T_\mathrm{a})}e^{\frac{2\left(\sqrt{\frac{k_\mathrm{d}}{h(d)}}(2T+T_\mathrm{a})+k_\mathrm{d}TT_\mathrm{a}\right)}{T-T_\mathrm{a}}}\right)$$
$$+\sqrt{\pi}\left(-4k_\mathrm{d}h(d)(T-T_\mathrm{a})-4\sqrt{k_\mathrm{d}h(d)}+h(d)\right)\mathrm{erf}\left(\frac{\sqrt{k_\mathrm{d}h(d)}(T-T_\mathrm{a})+1}{\sqrt{h(d)(T-T_\mathrm{a})}}\right)$$
$$+\sqrt{\pi}\left(h(d)(4k_\mathrm{d}T-1)+4\sqrt{k_\mathrm{d}h(d)}\right)\mathrm{erf}\left(\frac{T\sqrt{k_\mathrm{d}h(d)}+1}{\sqrt{h(d)T}}\right)+\sqrt{\pi}h(d)e^{-\frac{4k_\mathrm{d}}{\sqrt{k_\mathrm{d}h(d)}}}\mathrm{erf}\left(\frac{1-T\sqrt{k_\mathrm{d}h(d)}}{\sqrt{h(d)T}}\right)\Bigg] \tag{57}$$

$$E_{T_\mathrm{a}}^{(-)}(d,T) = \frac{1}{4k_\mathrm{d}\sqrt{k_\mathrm{d}h(d)}T_\mathrm{a}}\Bigg[(4k_\mathrm{d}-4k_\mathrm{d}\sqrt{k_\mathrm{d}h(d)}(T-T_\mathrm{a})+\sqrt{k_\mathrm{d}h(d)})\,\mathrm{erf}\left(\frac{1-\sqrt{k_\mathrm{d}h(d)}(T-T_\mathrm{a})}{\sqrt{h(d)(T-T_\mathrm{a})}}\right)$$
$$+\left(4k_\mathrm{d}-4Tk_\mathrm{d}\sqrt{k_\mathrm{d}h(d)}+\sqrt{k_\mathrm{d}h(d)}\right)\mathrm{erf}\left(\frac{T\sqrt{k_\mathrm{d}h(d)}-1}{\sqrt{h(d)T}}\right)$$
$$+e^{4\sqrt{\frac{k_\mathrm{d}}{h(d)}}}\sqrt{k_\mathrm{d}h(d)}\left(\mathrm{erf}\left(\frac{1+T\sqrt{k_\mathrm{d}h(d)}}{\sqrt{h(d)T}}\right)-\mathrm{erf}\left(\frac{1+\sqrt{k_\mathrm{d}h(d)}(T-T_\mathrm{a})}{\sqrt{h(d)(T-T_\mathrm{a})}}\right)\right)$$
$$+\frac{4k_\mathrm{d}\sqrt{h(d)(T-T_\mathrm{a})}\;e^{\frac{2\sqrt{k_\mathrm{d}h(d)}-\frac{1}{T-T_\mathrm{a}}}{h(d)}-k_\mathrm{d}(T-T_\mathrm{a})}}{\sqrt{\pi}}-\frac{4k_\mathrm{d}\sqrt{h(d)T}\;e^{\frac{2T\sqrt{k_\mathrm{d}h(d)}-1}{h(d)T}-k_\mathrm{d}T}}{\sqrt{\pi}}\Bigg] \tag{58}$$

Thus, the FIM is a 3×3 that can be written as:

$$\mathbf{J}(\boldsymbol{p}) \triangleq \mathbb{E}\left\{\frac{\partial \ln p(\mathbf{r})}{\partial \boldsymbol{p}}\;\frac{\partial \ln p(\mathbf{r})}{\partial \boldsymbol{p}}^T\right\} = -\mathbb{E}\left\{\frac{\partial^2 \ln p(\mathbf{r})}{\partial \boldsymbol{p}\,\partial \boldsymbol{p}^T}\right\}$$
$$= -\begin{bmatrix}\mathbb{E}\left\{\frac{\partial^2 \ln p(\mathbf{r})}{\partial x^2}\right\} & \mathbb{E}\left\{\frac{\partial^2 \ln p(\mathbf{r})}{\partial x\partial y}\right\} & \mathbb{E}\left\{\frac{\partial^2 \ln p(\mathbf{r})}{\partial x\partial z}\right\}\\ \mathbb{E}\left\{\frac{\partial^2 \ln p(\mathbf{r})}{\partial y\partial x}\right\} & \mathbb{E}\left\{\frac{\partial^2 \ln p(\mathbf{r})}{\partial x^2}\right\} & \mathbb{E}\left\{\frac{\partial^2 \ln p(\mathbf{r})}{\partial y\partial z}\right\}\\ \mathbb{E}\left\{\frac{\partial^2 \ln p(\mathbf{r})}{\partial z\partial x}\right\} & \mathbb{E}\left\{\frac{\partial^2 \ln p(\mathbf{r})}{\partial z\partial y}\right\} & \mathbb{E}\left\{\frac{\partial^2 \ln p(\mathbf{r})}{\partial z^2}\right\}\end{bmatrix}, \tag{61}$$

where the expectation is done with respect to $\mathbf{r}$. In other words the operator $\mathbb{E}\{\cdot\}$ applied to a generic function of $\mathbf{r}$, $g(\mathbf{r})$, means

$$\mathbb{E}\{g(\mathbf{r})\} = \sum_{n_1=1}^{+\infty}\frac{\lambda_1^{n_1}\,e^{-\lambda_1}}{n_1!}\sum_{n_2=1}^{+\infty}\frac{\lambda_2^{n_2}\,e^{-\lambda_2}}{n_2!}\cdots$$
$$\cdot\sum_{n_L=1}^{+\infty}\frac{\lambda_L^{n_L}\,e^{-\lambda_L}}{n_L!}g(n_1,n_2,\ldots,n_L)\,, \tag{62}$$

in accordance with (40). Thus, the elements of $\mathbf{J}(\boldsymbol{p})$ can be computed from (60) and (61) as follows. The elements on the main diagonal can be obtained by averaging the second order derivatives:

$$-\mathbb{E}\left\{\frac{\partial^2 \ln p(\mathbf{r})}{\partial x^2}\right\} = -\mathbb{E}\Bigg\{\sum_{l=1}^{L}\left(-\frac{n_l}{\lambda_l^2}\frac{\partial\lambda_l}{\partial x}\right)\frac{\partial\lambda_l}{\partial x}$$
$$\left.+\left(\frac{n_l}{\lambda_l}-1\right)\frac{\partial^2\lambda_l}{\partial x^2}\right\}$$
$$=\sum_{l=1}^{L}\left[\frac{\overbrace{\mathbb{E}\{n_l\}}^{=\lambda_l}}{\lambda_l^2}\left(\frac{\partial\lambda_l}{\partial x}\right)^2\right.$$
$$\left.-\left(\frac{\overbrace{\mathbb{E}\{n_l\}}^{=\lambda_l}}{\lambda_l}-1\right)\frac{\partial^2\lambda_l}{\partial x^2}\right]$$
$$=\sum_{l=1}^{L}\frac{1}{\lambda_l}\left(\frac{\partial\lambda_l}{\partial x}\right)^2, \tag{63}$$

and, by applying the same method with y and z in the place of x:

$$-\mathbb{E}\left\{\frac{\partial^2 \ln p(\mathbf{r})}{\partial y^2}\right\} = \sum_{l=1}^{L}\frac{1}{\lambda_l}\left(\frac{\partial\lambda_l}{\partial y}\right)^2 \tag{64}$$

$$-\mathbb{E}\left\{\frac{\partial^2 \ln p(\mathbf{r})}{\partial z^2}\right\} = \sum_{l=1}^{L}\frac{1}{\lambda_l}\left(\frac{\partial\lambda_l}{\partial z}\right)^2. \tag{65}$$

$$\mathbf{J}(\boldsymbol{p}) = \begin{bmatrix} \sum_{l=1}^{L} \frac{1}{\lambda_l} \left(\frac{\partial \lambda_l}{\partial x}\right)^2 & \sum_{l=1}^{L} \frac{1}{\lambda_l} \frac{\partial \lambda_l}{\partial x} \frac{\partial \lambda_l}{\partial y} & \sum_{l=1}^{L} \frac{1}{\lambda_l} \frac{\partial \lambda_l}{\partial x} \frac{\partial \lambda_l}{\partial z} \\ \sum_{l=1}^{L} \frac{1}{\lambda_l} \frac{\partial \lambda_l}{\partial y} \frac{\partial \lambda_l}{\partial x} & \sum_{l=1}^{L} \frac{1}{\lambda_l} \left(\frac{\partial \lambda_l}{\partial y}\right)^2 & \sum_{l=1}^{L} \frac{1}{\lambda_l} \frac{\partial \lambda_l}{\partial y} \frac{\partial \lambda_l}{\partial z} \\ \sum_{l=1}^{L} \frac{1}{\lambda_l} \frac{\partial \lambda_l}{\partial z} \frac{\partial \lambda_l}{\partial x} & \sum_{l=1}^{L} \frac{1}{\lambda_l} \frac{\partial \lambda_l}{\partial z} \frac{\partial \lambda_l}{\partial y} & \sum_{l=1}^{L} \frac{1}{\lambda_l} \left(\frac{\partial \lambda_l}{\partial z}\right)^2 \end{bmatrix} \tag{67}$$

The other elements can be obtained by averaging the mixed derivatives as follows:

$$\begin{aligned} -\mathbb{E}\left\{\frac{\partial^2 \ln p(\mathbf{r})}{\partial x \partial y}\right\} &= -\mathbb{E}\left\{\sum_{l=1}^{L}\left(-\frac{n_l}{\lambda_l^2}\frac{\partial \lambda_l}{\partial y}\right)\frac{\partial \lambda_l}{\partial x} \right. \\ &\qquad \left. + \left(\frac{n_l}{\lambda_l} - 1\right)\frac{\partial^2 \lambda_l}{\partial x\, \partial y}\right\} \\ &= \sum_{l=1}^{L}\left[\frac{\overbrace{\mathbb{E}\{n_l\}}^{=\lambda_l}}{\lambda_l^2}\frac{\partial \lambda_l}{\partial x}\frac{\partial \lambda_l}{\partial y}\right. \\ &\qquad \left. - \left(\frac{\overbrace{\mathbb{E}\{n_l\}}^{=\lambda_l}}{\lambda_l} - 1\right)\frac{\partial^2 \lambda_l}{\partial x\, \partial y}\right] \\ &= \sum_{l=1}^{L}\frac{1}{\lambda_l}\frac{\partial \lambda_l}{\partial x}\frac{\partial \lambda_l}{\partial y}\,, \end{aligned} \tag{66}$$

that can be extended to all the other combinations of coordinates. Thus, from (61), the FIM becomes (67).

ACKNOWLEDGMENT

I would like to thank Barbara Masini and the anonymous reviewers for their valuable comments, which have greatly enhanced the quality of this paper. I am indebted to Gianni Pasolini for his insightful discussions on the potential applications of molecular diffusion. I appreciate Andrea Conti and Davide Dardari for their assistance in understanding the fundamentals of localization. Special thanks go to Andrea Giorgetti for sparking my interest in the topic of joint sensing and communications. Finally, I am grateful to Oreste Andrisano, Roberto Verdone, and all my colleagues at WiLab for their unwavering support.

REFERENCES

[1] T. Wild, V. Braun, and H. Viswanathan, "Joint design of communication and sensing for beyond 5G and 6G systems," *IEEE Access*, vol. 9, pp. 30 845–30 857, 2021.

[2] S. D. Liyanaarachchi, T. Riihonen, C. B. Barneto, and M. Valkama, "Optimized waveforms for 5G–6G communication with sensing: Theory, simulations and experiments," *IEEE Transactions on Wireless Communications*, vol. 20, no. 12, pp. 8301–8315, 2021.

[3] L. Pucci, E. Paolini, and A. Giorgetti, "System-level analysis of joint sensing and communication based on 5G new radio," *IEEE Journal on Selected Areas in Communications*, vol. 40, no. 7, pp. 2043–2055, 2022.

[4] X. Fang, W. Feng, Y. Chen, N. Ge, and Y. Zhang, "Joint communication and sensing toward 6G: Models and potential of using mimo," *IEEE Internet of Things Journal*, vol. 10, no. 5, pp. 4093–4116, 2023.

[5] M. Ashraf, B. Tan, D. Moltchanov, J. S. Thompson, and M. Valkama, "Joint optimization of radar and communications performance in 6G cellular systems," *IEEE Transactions on Green Communications and Networking*, vol. 7, no. 1, pp. 522–536, 2023.

[6] R. Li, Z. Xiao, and Y. Zeng, "Towards seamless sensing coverage for cellular multi-static integrated sensing and communication," *IEEE Transactions on Wireless Communications*, pp. 1–1, 2023.

[7] F. Liu, Y.-F. Liu, A. Li, C. Masouros, and Y. C. Eldar, "Cramér-Rao bound optimization for joint radar-communication beamforming," *IEEE Transactions on Signal Processing*, vol. 70, pp. 240–253, 2022.

[8] F. Zabini, E. Paolini, W. Xu, and A. Giorgetti, "Joint sensing and communications in finite block-length regime," in *GLOBECOM 2022 - 2022 IEEE Global Communications Conference*, 2022, pp. 5595–5600.

[9] ——, "Joint sensing and communication with multiple antennas and bistatic configuration," in *2023 IEEE International Conference on Communications Workshops (ICC Workshops)*, 2023, pp. 1416–1421.

[10] M. Pierobon and I. F. Akyildiz, "Diffusion-based noise analysis for molecular communication in nanonetworks," *IEEE Transactions on Signal Processing*, vol. 59, no. 6, pp. 2532–2547, June 2011.

[11] M. Pierobon and I. F. Akyildiz, "Capacity of a diffusion-based molecular communication system with channel memory and molecular noise," *IEEE Transactions on Information Theory*, vol. 59, no. 2, pp. 942–954, Feb 2013.

[12] S. A. Salehi, H. Jiang, M. D. Riedel, and K. K. Parhi, "Molecular sensing and computing systems," *IEEE Transactions on Molecular, Biological and Multi-Scale Communications*, vol. 1, no. 3, pp. 249–264, Sept 2015.

[13] D. T. Gillespie, "The chemical Langevin equation," *The Journal of Chemical Physics*, vol. 113, no. 1, pp. 297–306, 2000. [Online]. Available: https://doi.org/10.1063/1.481811

[14] P. J. Thomas, D. J. Spencer, S. K. Hampton, P. Park, and J. P. Zurkus, "The diffusion-limited biochemical signal-relay channel," in *Advances in Neural Information Processing Systems 16*, S. Thrun, L. K. Saul, and B. Schölkopf, Eds. MIT Press, 2004, pp. 1263–1270. [Online]. Available: http://papers.nips.cc/paper/2522-the-diffusion-limited-biochemical-signal-relay-channel.pdf

[15] M. Pierobon and I. F. Akyildiz, "Capacity of a diffusion-based molecular communication system with channel memory and molecular noise," *IEEE Transactions on Information Theory*, vol. 59, no. 2, pp. 942–954, Feb 2013.

[16] B. Tepekule, A. E. Pusane, H. B. Yilmaz, C.-B. Chae, and T. Tugcu, "Isi mitigation techniques in molecular communication," *IEEE Transactions on Molecular, Biological and Multi-Scale Communications*, vol. 1, no. 2, pp. 202–216, 2015.

[17] Y. Huang, F. Ji, Z. Wei, M. Wen, X. Chen, Y. Tang, and W. Guo, "Frequency domain analysis and equalization for molecular communication," *IEEE Transactions on Signal Processing*, vol. 69, pp. 1952–1967, 2021.

[18] A. C. Heren, H. B. Yilmaz, C.-B. Chae, and T. Tugcu, "Effect of degradation in molecular communication: Impairment or enhancement?" *IEEE Transactions on Molecular, Biological and Multi-Scale Communications*, vol. 1, no. 2, pp. 217–229, 2015.

[19] Y. Deng, A. Noel, W. Guo, A. Nallanathan, and M. Elkashlan, "Analyzing large-scale multiuser molecular communication via 3-D stochastic geometry," *IEEE Transactions on Molecular, Biological and Multi-Scale Communications*, vol. 3, no. 2, pp. 118–133, June 2017.

[20] F. Zabini, "Spatially distributed molecular communications: An asynchronous stochastic model," *IEEE Communications Letters*, vol. 22, no. 7, pp. 1326–1329, July 2018.

[21] F. Zabini, G. Pasolini, C. De Castro, and O. Andrisano, "On molecular communications via diffusion with multiple transmitters and multiple receivers," in *2018 IEEE Global Communications Conference (GLOBECOM)*, Dec 2018, pp. 206–212.

[22] F. Zabini, "Spatially distributed molecular communications via diffusion: Second-order analysis," *IEEE Transactions on Molecular, Biological and Multi-Scale Communications*, vol. 5, no. 2, pp. 112–138, 2019.

[23] E. Dinc and O. B. Akan, "Theoretical limits on multiuser molecular communication in internet of nano-bio things," *IEEE Transactions on NanoBioscience*, vol. 16, no. 4, pp. 266–270, 2017.

[24] L. Felicetti, M. Femminella, and G. Reali, "Congestion control in molecular cyber-physical systems," *IEEE Access*, vol. 5, pp. 10 000–10 011, 2017.

[25] B. C. Akdeniz, N. A. Turgut, H. B. Yilmaz, C.-B. Chae, T. Tugcu, and A. E. Pusane, "Molecular signal modeling of a partially counting absorbing spherical receiver," *IEEE Transactions on Communications*, vol. 66, no. 12, pp. 6237–6246, 2018.

[26] F. Z. Zabini and B. M. Masini, "Performance limits of spatially distributed molecular communications with receiver saturation," *IEEE Transactions on Molecular, Biological and Multi-Scale Communications*, vol. 9, no. 1, pp. 94–99, 2023.

[27] S. Malik, J. Singh, R. Goyat, Y. Saharan, V. Chaudhry, A. Umar, A. A. Ibrahim, S. Akbar, S. Ameen, and S. Baskoutas, "Nanomaterials-based biosensor and their applications: A review," *Heliyon*, vol. 9, no. 9, p. e19929, 2023. [Online]. Available: https://www.sciencedirect.com/science/article/pii/S2405844023071372

[28] A. Yusuf, A. R. Z. Almotairy, H. Henidi, O. Y. Alshehri, and M. S. Aldughaim, "Nanoparticles as drug delivery systems: A review of the implication of nanoparticles physicochemical properties on responses in biological systems," *Polymers*, vol. 15, no. 7, 2023. [Online]. Available: https://www.mdpi.com/2073-4360/15/7/1596

[29] C.-Y. Hsu, A. M. Rheima, M. M. Kadhim, N. N. Ahmed, S. H. Mohammed, F. H. Abbas, Z. T. Abed, Z. M. Mahdi, Z. S. Abbas, S. K. Hachim, F. K. Ali, Z. H. Mahmoud, and E. Kianfar, "An overview of nanoparticles in drug delivery: Properties and applications," *South African Journal of Chemical Engineering*, vol. 46, pp. 233–270, 2023. [Online]. Available: https://www.sciencedirect.com/science/article/pii/S102691852300080X

[30] F. Calí, L. Fichera, G. Trusso Sfrazzetto, G. Nicotra, G. Sfuncia, E. Bruno, L. Lanzanó, I. Barbagallo, G. Li-Destri, and N. Tuccitto, "Fluorescent nanoparticles for reliable communication among implantable medical devices," *Carbon*, vol. 190, pp. 262–275, 2022. [Online]. Available: https://www.sciencedirect.com/science/article/pii/S0008622322000161

[31] D. Bhatia, S. Paul, T. Acharjee, and S. S. Ramachairy, "Biosensors and their widespread impact on human health," *Sensors International*, vol. 5, p. 100257, 2024. [Online]. Available: https://www.sciencedirect.com/science/article/pii/S2666351123000311

[32] A. Etemadi, M. Farahnak-Ghazani, H. Arjmandi, M. Mirmohseni, and M. Nasiri-Kenari, "Abnormality detection and localization schemes using molecular communication systems: A survey," *IEEE Access*, vol. 11, pp. 1761–1792, 2023.

[33] M. Khalid, O. Amin, S. Ahmed, and M.-S. Alouini, "System modeling of virus transmission and detection in molecular communication channels," in *2018 IEEE International Conference on Communications (ICC)*, 2018, pp. 1–6.

[34] R. Mosayebi, W. Wicke, V. Jamali, A. Ahmadzadeh, R. Schober, and M. Nasiri-Kenari, "Advanced target detection via molecular communication," in *2018 IEEE Global Communications Conference (GLOBECOM)*, 2018, pp. 1–7.

[35] R. Mosayebi, A. Ahmadzadeh, W. Wicke, V. Jamali, R. Schober, and M. Nasiri-Kenari, "Early cancer detection in blood vessels using mobile nanosensors," *IEEE Transactions on NanoBioscience*, vol. 18, no. 2, pp. 103–116, 2019.

[36] L. Khaloopour, M. Mirmohseni, and M. Nasiri-Kenari, "Theoretical concept study of cooperative abnormality detection and localization in fluidic-medium molecular communication," *IEEE Sensors Journal*, vol. 21, no. 15, pp. 17 118–17 130, 2021.

[37] Y. Chen, P. Kosmas, P. S. Anwar, and L. Huang, "A touch-communication framework for drug delivery based on a transient microbot system," *IEEE Transactions on NanoBioscience*, vol. 14, no. 4, pp. 397–408, 2015.

[38] S. Shi, Y. Yan, J. Xiong, U. K. Cheang, X. Yao, and Y. Chen, "Nanorobots-assisted natural computation for multifocal tumor sensitization and targeting," *IEEE Transactions on NanoBioscience*, vol. 20, no. 2, pp. 154–165, 2021.

[39] S. Ghavami and F. Lahouti, "Abnormality detection in correlated gaussian molecular nano-networks: Design and analysis," *IEEE Transactions on NanoBioscience*, vol. 16, no. 3, pp. 189–202, 2017.

[40] H. Arjmandi, A. Ahmadzadeh, R. Schober, and M. Nasiri Kenari, "Ion channel based bio-synthetic modulator for diffusive molecular communication," *IEEE Transactions on NanoBioscience*, vol. 15, no. 5, pp. 418–432, 2016.

[41] H. Arjmandi, V. Jamali, A. Ahmadzadeh, A. Burkovski, R. Schober, and M. N. Kenari, "Ion pump based bio-synthetic modulator model for diffusive molecular communications," in *2016 IEEE 17th International Workshop on Signal Processing Advances in Wireless Communications (SPAWC)*, 2016, pp. 1–6.

[42] M. J. Moore, T. Nakano, A. Enomoto, and T. Suda, "Measuring distance from single spike feedback signals in molecular communication," *IEEE Transactions on Signal Processing*, vol. 60, no. 7, pp. 3576–3587, 2012.

[43] X. Wang, M. D. Higgins, and M. S. Leeson, "Distance estimation schemes for diffusion based molecular communication systems," *IEEE Communications Letters*, vol. 19, no. 3, pp. 399–402, 2015.

[44] M. Turan, B. C. Akdeniz, M. S. Kuran, H. B. Yilmaz, I. Demirkol, A. E. Pusane, and T. Tugcu, "Transmitter localization in vessel-like diffusive channels using ring-shaped molecular receivers," *IEEE Communications Letters*, vol. 22, no. 12, pp. 2511–2514, 2018.

[45] Y. Miao, W. Zhang, and X. Bao, "Levenberg–Marquardt method-based cooperative source localization in SIMO molecular communication via diffusion systems," *IEEE Transactions on Molecular, Biological and Multi-Scale Communications*, vol. 8, no. 4, pp. 229–238, 2022.

[46] S. Kumar, "Nanomachine localization in a diffusive molecular communication system," *IEEE Systems Journal*, vol. 14, no. 2, pp. 3011–3014, 2020.

[47] A. Kumar, A. Yadav, and S. Kumar, "Rectangular concentration-based nanomachine localization in molecular communication networks with unknown emission time," *IEEE Transactions on Molecular, Biological and Multi-Scale Communications*, vol. 9, no. 4, pp. 472–477, 2023.

[48] L. Khaloopour, M. Mirmohseni, and M. Nasiri-Kenari, "Joint sensing, communication, and localization of a silent abnormality using molecular diffusion," *IEEE Internet of Things Journal*, vol. 10, no. 6, pp. 4871–4882, 2023.

[49] Y. Wang and W. Xiong, "Anchor-based three-dimensional localization using range measurements," in *2012 8th International Conference on Wireless Communications, Networking and Mobile Computing*, 2012, pp. 1–5.

[50] F. Zabini and B. M. Masini, "Performance limits in 3d localization via molecular diffusion," in *to be presented at 2024 IEEE International Symposium on Information Theory (ISIT)*, 2024.

[51] N. V. Sabu, A. K. Gupta, N. Varshney, and A. Jindal, "Channel characterization and performance of a 3-D molecular communication system with multiple fully-absorbing receivers," *IEEE Transactions on Communications*, vol. 71, no. 2, pp. 714–727, 2023.

[52] H. B. Yilmaz, A. C. Heren, T. Tugcu, and C. B. Chae, "Three-dimensional channel characteristics for molecular communications with an absorbing receiver," *IEEE Communications Letters*, vol. 18, no. 6, pp. 929–932, June 2014.

[53] V. Jamali, A. Ahmadzadeh, W. Wicke, A. Noel, and R. Schober, "Channel modeling for diffusive molecular communication—a tutorial review," *Proceedings of the IEEE*, vol. 107, no. 7, pp. 1256–1301, July 2019.

[54] A. Gohari, M. Mirmohseni, and M. Nasiri-Kenari, "Information theory of molecular communication: Directions and challenges," *IEEE Transactions on Molecular, Biological and Multi-Scale Communications*, vol. 2, no. 2, pp. 120–142, Dec 2016.

[55] J. F. Kingman, *Poisson Processes*, U. Oxford University Press, Ed., 1993.

[56] O. Macchi, "Stochastic point processes and multicoincidences," *IEEE Trans. Inf. Theory*, vol. 17, no. 1, pp. 2–7, Jan. 1971.

[57] ——, "The coincidence approach to stochastic point processes," *Adv. Appl. Probab.*, vol. 7, no. 1, pp. 83–122, 1975. [Online]. Available: http://www.jstor.org/stable/1425855

[58] S. N. Chiu, D. Stoyan, W. Kendall, and J. Mecke, *Stochastic Geometry and Its Applications, 3rd Edition*, 3rd ed., Ed. John Wiley and Sons, 2013.

[59] N. V. Sabu, N. Varshney, and A. K. Gupta, "3-D diffusive molecular communication with two fully-absorbing receivers: Hitting probability and performance analysis," *IEEE Transactions on Molecular, Biological and Multi-Scale Communications*, vol. 6, no. 3, pp. 244–249, 2020.

Flavio Zabini (M'13) received the Laurea (*summa cum laude*) in telecommunications engineering and the Ph.D. in electronic engineering and computer science from the University of Bologna, Italy, in 2004 and 2010, respectively. In 2004, he developed his master's thesis at the University of California San Diego, La Jolla. In 2008, he was a Visiting Student with the DoCoMo Eurolabs of Munich, Germany. From 2013 to 2014, he was a Post-Doctoral Fellow with the German Aerospace Center, Cologne, Germany. He was with the IEIIT-Bo of CNR. He is currently a Researcher with the University of Bologna. His current research interests include stochastic sampling, molecular communications, and joint sensing and communications. He served as an associate Editor for the IEEE Communication Letters and the KSII Transactions on Internet and Information Systems.